Dissertation

Applications of Liquid Biopsy in Breast Cancer

submitted by

Dr. med. univ. Christoph Suppan

for the Academic Degree of

Doctor of Medical Science
(Dr. scient. med.)

at the

Medical University of Graz

Department of Internal Medicine
Clinical Division of Oncology

under the Supervision of

Assoz. Prof. Priv. Doz. Dr. med. univ. et scient. med. Marija Balic

2021

Declaration

I hereby declare that this thesis is my own original work and that I have fully acknowledged by name all of those individuals and organisations that have contributed to the research for this thesis. Due acknowledgement has been made in the text to all other material used. Throughout this thesis and in all related publications I followed the "Guidelines of the Medical University of Graz on Good Scientific Practice.

Graz, March 2021

Disclosures

One part of the dissertation has been published in the following article:

Suppan C[1], Brcic I[2], Tiran V[3], Mueller HD[1], Posch F[1], Auer M[4], Ercan E[4], Ulz P[4], Cote RJ[5], Datar RH[5], Dandachi N[1], Heitzer E[4] and Balic M[1]

Untargeted Assessment of Tumor Fractions in Plasma for Monitoring and Prognostication from Metastatic Breast Cancer Patients Undergoing Systemic Treatment. Cancers (Basel). 2019;11(8).

[1] Clinical Division of Oncology, Department of Internal Medicine, Medical University of Graz, 8036 Graz, Austria

[2] Institute of Pathology, Medical University of Graz, 8010 Graz, Austria

[3] Department of Internal Medicine III with Haematology, Medical Oncology, Haemostaseology, Infectiology and Rheumatology, Oncologic Center, Salzburg Cancer Research Institute - Laboratory for Immunological and Molecular Cancer Research (SCRI-LIMCR), Paracelsus Medical University Salzburg, Salzburg, Austria.

[4] Institute of Human Genetics, Diagnostic and Research Center for Molecular Biomedicine, Medical University of Graz, 8010 Graz, Austria

[5] Department of Pathology, University of Miami Miller School of Medicine, Miami, FL 33136, USA

Acknowledgements

I would like to thank many people who supported me during this work – with their time, expertise and lasting patience.

First of all I would like to express my deepest gratitude to Prof. Marija Balic who very much encouraged me from day one. None of this would have been possible without her excellent mentorship and patience throughout my residency and on my path to becoming a medical oncologist. I am looking forward to further establish the breast cancer program at our Division of Oncology together with her.

I would also like to express much thanks to Nadia Dandachi for her deep support on many occasions, given her comprehensive understanding of statistics and molecular biology. I am looking forward to many more research meetings in our “souterrain”.

Also, I would like to express further thanks to Prof. Ellen Heitzer and her team. This work is, above all, the result of an outstanding collaboration with the Institute of Human Genetics. I am excited for ongoing collaboration in the future.

I would also like to express much gratitude to my former supervisor Prof. Herbert Stöger for his motivating words and introduction to the field of oncology, as well as Prof. Philipp Jost, current head of the Division of Oncology, for his inspiring character and giving me the last push to finalize this work.

Last but not least, thank you to my family and friends who make my life better every day.

This work was supported by the Christian Doppler Research Fund for Liquid Biopsies for Early Detection of Cancer**,** by the Federal Ministry of Digital and Economic Affairs and by Novartis.

The author received support by the Medical University of Graz through the Doctoral School Molecular Medicine and Inflammation.

Table of Contents

List of Abbreviations

ARMS ..... *amplification-refractory mutation system*
BEAMing ..... *Beads, Emulsion, Amplification, Magnetics digital PCR*
BRCA1 ..... *Breast Cancer 1*
BRCA2 ..... *Breast Cancer 2*
CA15-3 ..... *Cancer Antigen 15-3*
CDK4/6 ..... *cyclin-dependent protein kinases 4 and 6*
CEA ..... *carcinoembryonic antigen*
cfDNA ..... *cell-free DNA*
CTCs ..... *circulating tumor cells*
ctDNA ..... *circulating tumor DNA*
EMT ..... *epithelial-mesenchymal transition*
EpCAM ..... *epithelial cell adhesion molecule*
ER ..... *estrogen receptor*
ERBB-2 ..... *erb-b2 receptor tyrosine kinase 2*
ESR1 ..... *Estrogen Receptor 1*
FDA ..... *U.S. Food and Drug Administration*
Her-2 ..... *human epidermal growth factor receptor 2*
HR ..... *hormone-receptor*
LINE1 ..... *long interspersed nuclear elements*
mFAST-SeqS ..... *2.1.3 Modified Fast Aneuploid Screening Test-Sequencing System*
NST ..... *No specific type*
OS ..... *overall survival*
PARP ..... *Poly(adenosine diphosphate-ribose) polymerases*
pCR ..... *pathologic complete response*, *pathological complete response*
PD-L1 ..... *programmed death ligand 1*
PFS ..... *progression-free survival*
PI2 ..... *phosphatidylinositol 4,5- bisphosphate*
PI3K ..... *Phosphatidylinositol 3-kinase*
PIP2 ..... *phosphatidylinositol 4,5- bisphosphate*
PIP3 ..... *phosphatidylinositol 3,4,5-triphosphate*
PR ..... *progesterone receptor*
qPCR ..... *quantitative real-time Polymerase chain reaction*
SafeSeqS ..... *Safe Sequencing System*
SCNAs ..... *Somatic copy number alterations*
SiMSen-Seq ..... *simple, multiplexed, PCR-based barcoding of DNA for sensitive mutation detection using sequencing*
VAF ..... *variant allele frequencies*

List of Figures

List of Tables

Abstract

Background

The analysis of tumor components in blood such as circulating tumor cells (CTCs) or circulating tumor DNA (ctDNA) represents an easy, fast, non-invasive and cost-effective tool for both the assessment of tumor dynamics during the treatment of metastatic breast cancer patients and the detection of targetable alterations.

Methods

In a first step, tumor fractions in plasma of metastatic breast cancer patients were assessed using the untargeted mFAST-SeqS method from 127 serial blood samples. Resulting z-scores for the ctDNA were compared to tumor fractions established with the ichorCNA algorithm and associated with the clinical outcome. Then, we compared the performance of ctDNA, CTCs detected by size-based CTC microfilter enrichment, and blood-based parameters CEA and CA15-3. In a second step, plasma samples and tumor tissue from 69 patients with metastatic hormone-receptor positive breast cancer were analyzed for *PIK3CA* hotspot mutations. A high-resolution SiMSen-Seq method was used for plasma samples covering 11 *PIK3CA* mutations. Again, mFAST-SeqS was used to estimate the tumor fractions in the plasma samples.

Results

We observed a close correlation between mFAST-SeqS z-scores and ichorCNA ctDNA quantifications. Patients with mFAST-SeqS z-scores above three (34.5%) showed significantly worse overall (*p=0.014)* and progression-free survival (*p=0.018*) compared to patients with lower values. The baseline CTC count, CEA, and CA15-3 had no prognostic impact on the outcome of patients in the analyzed cohort. *PIK3CA* mutations were detected in 46.1% of the tissue samples and in 50.7% of the plasma samples. In 7 patients, *PIK3CA* mutations were found only in plasma. In 5 patients, such mutations found in tissue were not detectable in ctDNA, 2 of which had a low tumor fraction. Together, in 33/67 plasma samples without detectable *PIK3CA* mutations, 18 samples had elevated tumor fraction, implicating true negative results. In the remaining 15 patients with low tumor fraction, additional tissue analysis was needed.

Conclusion

Here, the prognostic impact of ctDNA levels detected with mFAST-SeqS demonstrates a tool to assess the ctDNA fraction without prior knowledge of the genetic landscape of the tumor. In addition, SiMSen-Seq-based detection of *PIK3CA* mutations in plasma shows advantageous concordance with the tissue analyses. A combination with an untargeted,

mutation-independent approach for detecting ctDNA fractions may confirm a negative *PIK3CA* result and thereby enhance the performance of the SiMSen-Seq test.

Zusammenfassung

Hintergrund

Der Nachweis von Tumorkomponenten im Blut wie zirkulierende Tumorzellen (CTCs) oder zirkulierende Tumor – DNA (ctDNA) stellt ein einfaches, schnelles, nichtinvasives und kosteneffektives Verfahren dar zur Bestimmung der Tumordynamik unter laufender Therapie und der Detektion zielgerichteter Alterationen bei Patientinnen mit metastasiertem Mammakarzinom.

Methoden

In einem ersten Schritt wurden Tumorfraktionen im Plasma von Patientinnen mit metastasiertem Mammakarzinom mittels mFAST-SeqS aus 127 Blutproben bestimmt. Die ermittelten z-Scores für ctDNA wurden mit durch ichorCNA ermittelte Tumorfraktionen verglichen und mit klinischen Überlebensdaten assoziiert. Anschließend wurde die Vorhersagekraft von ctDNA, CTCs, die durch ein größenbasiertes Mikrofilter – Anreicherungsverfahren detektiert wurden mit den blutbasierten Parametern CEA und CA 15-3 verglichen. In einem zweiten Schritt wurden Plasmaproben und Tumorgewebe von 69 Patientinnen mit hormonrezeptorpositivem Mammakarzinom auf das Vorliegen von *PIK3CA* – Mutationen untersucht. Für die Analyse der Plasmaproben wurde ein hochauflösendes SiMSen-Seq zum Nachweis von 11 *PIK3CA* – Mutationen angewandt. Zusätzlich wurde die mFAST-SeqS – Methode zur groben Abschätzung der im Plasma enthaltenen Tumorfraktionen verwendet.

Ergebnisse

Wir konnten eine enge Übereinstimmung zwischen mit mFAST-SeqS ermittelten z-Scores und Quantifizierung von ctDNA ermitteln. Patientinnen mit einem z-Score > 3 (34.5%) hatten ein signifikant schlechteres Gesamtüberleben (*p=0.014)* sowie progressionsfreies Überleben (*p=0.018*) im Vergleich zu Patientinnen mit niedrigeren Werten. Die CTC – Anzahl zu Beginn, CEA und CA 15-3 hatten keinen prognostischen Einfluss auf das Outcome der Patientinnen in der analysierten Kohorte.

PIK3CA - Mutationen wurden in 46.1% der Gewebsproben und in 50.7% der Plasmaproben detektiert. In 7 Patientinnen wurden *PIK3CA* – Mutationen nur im Plasma nachgewiesen. In 5 Patientinnen wurden Mutationen, die im Gewebe nachweisbar waren, nicht durch ctDNA detektiert, 2 davon hatten eine niedrige Tumorfraktion. Von insgesamt 33 aus 67 Plasmaproben, in denen keine *PIK3CA* – Mutationen detektiert werden konnten, war in 18 Proben eine erhöhte Tumorfraktion nachweisbar. Bei den verbliebenen 15 Patientinnen mit niedriger Tumorfraktion war eine zusätzliche Gewebstestung notwendig.

Schlussfolgerung

Der prognostische Einfluss detektierter ctDNA anhand der mFAST-SeqS – Methode wird demonstriert und bestätigt diese als Möglichkeit zur Konzentrationsbestimmung von ctDNA ohne vorherige Kenntnis der genetischen Zusammensetzung des Tumors.

Die SimSen-Seq – basierte Detektion von *PIK3CA* – Mutationen im Plasma zeigt eine vorteilhafte Konkordanz mit der Gewebsanalyse. Die Kombination mit einem nicht zielgerichteten, mutationsunabhängigen Verfahren zur Detektion von *PIK3CA* – Mutationen kann ein negatives *PIK3CA* – Ergebnis bestätigen und dadurch die Validität der SiMSen-Seq – Testung erhöhen.

1 Introduction

Breast cancer is still the most common diagnosed cancer in women worldwide and the third leading cause of cancer-related deaths in Europe and the United States of America (1). At diagnosis, approximately 60% are confined to the breast and 30% have already spread to the regional lymph nodes. Under 10% of newly diagnosed breast cancers have already metastasized into distant organs and thus count for an incurable disease. More than a half of all breast cancers are diagnosed through screening mammography. One third is diagnosed through palpation of the breast (2). The clinical presentation of breast cancer may include palpable axillary mass, breast skin erythema, asymmetry of the breast or nipple inversion. The final diagnosis has to be histologically confirmed.

1.1 Breast Cancer – Basics

1.1.1 Pathology

Breast cancer histology is in 50 – 75% invasive ductal carcinoma, also known as no specific type (NST), in 5 – 15% invasive lobular carcinoma and mixed or other histologies in remaining cases of the patients (3, 4).

In general, there are two main molecular targets in breast cancer of prognostic and therapeutic relevance: First, there is the estrogen receptor alpha (ER) which is expressed in about 70% of invasive breast cancers and can activate growth pathways in breast cancer cells after being activated by estrogen. This steroid hormone receptor often shows up together with the expression of the progesterone receptor (PR). Tumors expressing one of these receptors in at least 1% are therefore defined as hormone-receptor (HR) positive. Thus, downregulation of estrogen receptor signaling by endocrine therapy is the key management when treating hormone receptor positive breast cancer patients (5).

The second main molecular target is the epidermal growth factor 2 (ERBB-2 or Her-2). A transmembrane receptor tyrosine kinase, that is overexpressed in approximately 20% of invasive breast cancers. It correlates with poor prognosis in the absence of systemic therapy. Tumors with amplification or overexpression of Her-2 are ERBB-2 positive or Her-2 positive. Targeting this receptor by antibody therapies or small molecule tyrosine kinase inhibitors is the key management in the treatment of ERBB-2 positive breast cancer patients (6-9).

The third breast cancer subgroup is characterized by the lack of overexpression of these main molecular targets and defined as triple-negative breast cancer. It is the smallest group and

occurs in approximately 15% of invasive breast cancers, being the most aggressive subtype and showing a high recurrence rate in the first three to five years after diagnosis (10, 11).

1.1.2 Molecular Classification

Regarding the heterogeneity of breast cancer microarray analyses have identified gene expression profiles allowing further classification of intrinsic subtypes. These breast cancer subtypes are associated with patient survival and differ in expression of hormone receptors and Her-2 (12-14).

1.1.2.1 Luminal subtypes

Luminal A and luminal B-expressing genes are very similar to luminal epithelium of the breast. They are the most common subtypes with expression of ER and PR. Luminal A tumors are characterized by high expression of ER-related genes, low occurrence of Her-2 – expression and low proliferation rates. Luminal A tumors are the most common subtype and related to the best prognosis in breast cancer patients (15-17). Luminal B tumors have lower ER expression, different expression of Her-2 and higher proliferation rates being associated with a worse prognosis (17).

1.1.2.2 Her2-enriched

This subtype comes up in 10 – 15 % of breast cancers and is characterized by high expression of Her-2 and proliferation-gene clusters as well as low expression of luminal clusters. Her-2 enrichment is a predictive factor to response to Her-2-targeted therapy.

1.1.2.3 ER-negative subtypes

The genomic profile is defined by the absence of ER expression. The most common type is the basal-like subtype with a tendency towards the basal epithelial cells of normal breast cells. It is typically defined as triple negative characterized by low luminal and Her-2-expression (12, 15).

1.1.3 Prognosis

Treatment options, prevalence and prognosis depend on breast cancer subtypes and stage. Stage I breast cancer is defined by a breast tumor smaller than 2 cm without lymph node involvement. It is correlated with a good prognosis and 5-year breast-cancer specific survival

of 99% for hormone receptor positive, 94% for Her2 positive and 85% for triple negative tumors. In metastatic setting or stage IV triple negative breast cancer patients have the worst prognosis: with a median overall-survival of 12 to 14 months compared to approximately five years in HR- or Her-2 positive patients (18-21).

1.1.4 Treatment Algorithms – nonmetastatic setting

Therapy strategies in nonmetastatic breast cancer consist of local therapy, systemic therapy and postoperative radiation. Local therapy includes surgical resection of the primary tumor with or without removing axillary lymph nodes. Systemic therapy eradicates tumor cells from the breast as well as circulating micrometastases. Its primary goal is to prevent recurrent disease. In general, it can be given pre- or postoperative and may include chemotherapy, endocrine therapy and Her-2 directed antibody drugs depending on the subtype.

1.1.4.1 Preoperative Treatment

Preoperative systemic treatment is not only used for locally advanced or inflammatory disease but has also been accepted as a treatment option for lower stage breast cancer. Downsizing the tumor in order to enhance the rate of breast conserving therapy is the main goal of preoperative systemic treatment. Moreover it may give prognostic information when under systemic therapy by assessing therapy response. Pathological complete response (pCR) is a surrogate marker for survival for the majority of breast cancer subtypes (22, 23).

1.1.4.2 Endocrine Therapy

In HR-positive breast cancer endocrine therapy as an oral antiestrogen medication is a standard procedure. Depending on the menopausal status of women there is Tamoxifen and the group of aromatase inhibitors: Tamoxifen is a selective estrogen receptor modulator that inhibits the binding of estrogen to the receptor and is used in pre- and postmenopausal patients. Whereas aromatase inhibitors target the conversion of androgens to estrogen and are effective in postmenopausal women. They can be also used in women with medical ovarian suppression or oophorectomy (24)

1.1.4.3 Chemotherapy and Her-2-targeted therapy

The addition of adjuvant chemotherapy in HR-positive breast cancer patients depends on clinicopathological features and might reduce breast cancer mortality (25). A decision may be

guided by RNA-based genomic risk scores and needs to be discussed individually with every single patient. When hormone receptor positive endocrine therapy is also part of standard treatment. In Her-2 positive breast cancer, systemic therapy includes the monoclonal antibody trastuzumab targeting the extracellular domain of Her-2. This is combined with chemotherapy for several weeks depending on the tumor stage, and given as monotherapy up to 12 months of treatment (26). In higher risk patients the antibody drug pertuzumab is combined with trastuzumab (27).
For postoperative treatment neratinib as a tyrosine kinase inhibitor and the antibody-drug-conjugate trastuzumab-emtansine are available (28, 29). Triple negative breast cancer in nonmetastatic setting must be treated with chemotherapy (30).

1.1.5 Treatment Algorithms – metastatic setting

The median overall survival rate in metastatic breast cancer patients differs between the different subtypes. Visceral and/or brain metastasis or multiple metastatic sites are often correlated with a worse prognosis. Whereas bone-only disease, younger age or a good performance status are factors that are more likely to improve prognosis (2). Currently, breast cancer in metastatic setting remains uncurable. The goal is prolonging life and symptom palliation. Therapy strategies in metastatic breast cancer are comparable to the adjuvant/neoadjuvant setting. Due to less toxicity and improved quality of life single agent chemotherapy is preferred over combination therapies (31, 32).

1.1.5.1 ER – positive

New treatment options have become available over the past years aiming to prolong endocrine sensitivity and survival in these patients. By focusing on pathways responsible for the development of endocrine resistance the initiation of chemotherapy may also be delayed.

1.1.5.1.1 CDK4/6 – Inhibition

Resistance mechanisms to endocrine therapy are often linked to activation of signal transduction pathways involved in cell cycle regulation. Binding of Cyclin D1 to cyclin-dependent protein kinases 4 and 6 (CDK4/6) results in cell cycle progression at the G1/S boundary. Therefore, inhibition of CDK4/6 induces growth arrest and due to a crosstalk between steroid hormone receptors represents a successful target together with endocrine therapy (33).

Currently, the CDK4/6-inhibitors abemaciclib, palbociclib and ribociclib are approved for treatment in combination with endocrine therapy. Several studies showed a significant improvement in progression-free survival and overall-survival compared to endocrine therapy alone (21, 34-42).

1.1.5.1.2 PI3K/AKT/mTOR pathway

After the introduction of CDK 4/6 inhibitors, targeted signal-transduction pathways have been established (43). Phosphatidylinositol 3-kinases (PI3Ks) are among the most important targets, apparently mediating the conversion of phosphatidylinositol 4,5- bisphosphate (PIP2) to phosphatidylinositol 3,4,5-triphosphate (PIP3) (44). The PI3K/AKT/mTOR pathway's ensuing upregulation plays a critical role in the essential process of disease progression including cell growth, proliferation, metabolism, and invasion (45).

In breast cancer, the PI3K/AKT/mTOR signaling pathway can be altered by different mechanisms. In approximately one third of early breast cancers activating mutations in the helical or kinase domain of *PIK3CA* can be found (45 % in luminal A, 29 % in luminal B, 39 % in HER2-enriched, and 9 % in the basal carcinomas) (46, 47). Similar rates of mutations can be found in metastatic breast cancer although fewer data is available (46).

Recent data suggests that *PIK3CA* alterations have an adverse impact on the prognosis of HR-positive disease and may play a role in endocrine resistance (48-50). Several drugs targeting the PI3 kinase pathway have been tested, but to date, only in the SOLAR-1 phase III trial, a clinically meaningful benefit of adding an α-specific PI3K inhibitor (alpelisib) was demonstrated with an acceptable tolerability profile (51). In this trial, only a minor proportion of patients was pretreated with CDK4/6 inhibitors. Still the benefit of PI3K inhibition in this patient's subset was confirmed in phase II BYLieve study (52). With this data in hand, the importance of the *PIK3CA*, encoding for the α-isoform of the catalytic subunit of the class IA PI3K kinase as a biomarker was postulated; the best testing approach, however, remains elusive. The stability of mutations over the course of the disease was only recently addressed by Mosele et al. (49). Prospective collection of metastatic tissue is ongoing in several large clinical trials such as AURORA (Aiming to Understand the Molecular Aberrations in Metastatic Breast Cancer, NCT02102165) (53). As tissue from metastatic sites may not always be available, interest in liquid biopsy techniques has grown. In the SOLAR-1 trial in parallel to the tissue-based detection, cell-free DNA was analyzed for the presence of *PIK3CA* mutations. Along with the approval of alpelisib, the U.S. Food and Drug Administration (FDA) has approved the companion diagnostic test therascreen® PIK3CA RGQ PCR Kit (QIAGEN

Manchester, Ltd.), to select patients who have *PIK3CA* mutations in tumor tissue specimens and/or in ctDNA isolated from plasma specimens.

1.1.5.2 Her-2 positive

In Her-2 positive metastatic disease first line therapy includes chemotherapy in combination with trastuzumab and pertuzumab (20), followed by the antibody-drug-conjugate trastuzumab-emtansine as a second line therapy (54, 55). In later lines, trastuzumab based therapy strategies in combination with chemotherapy or endocrine therapy in case of hormone receptor positive disease are standard.

1.1.5.3 Triple negative

Metastatic triple negative breast cancer is correlated with the worst prognosis in all breast cancer types. In approximately 40% of the patients, whose tumors are programmed death ligand 1 (PD-L1) positive on immune cells, the PD-L1 inhibitor atezolizumab in combination with nab-Paclitaxel is currently the preferred first-line therapy and showed an impressive overall survival benefit over nab-Paclitaxel alone (56).

1.1.6 Genomic and genetic testing

The presence of germline mutations in *BRCA1* and *BRCA2*, the two autosomal dominant breast cancer susceptibility genes, is associated with an elevated risk of developing breast or ovarian cancer (57).

Approximately 5% of breast cancer patients in metastatic setting are carrier of *BRCA1* or *BRCA2*. At the same time these patients often show having a strong family history, being at younger age or having breast cancer with triple negative histology. These tumor-suppressor genes encode proteins involved in the DNA-repair of double-strand breaks by homologous recombination. Poly(adenosine diphosphate-ribose) polymerases (PARP) play a role in the repair of single-strand breaks representing a target for inhibition. At the moment there are two approved PARP inhibitors (olaparib, talazoparib) available treating patients with metastatic breast cancer carrying a germline *BRCA1* or *BRCA2* mutation (58-60).

The presence of mismatch repair deficiency or high microsatellite instability is another alteration which occurs in 1% of patients and may be indicated for the use of a checkpoint immunotherapy (61). At the moment it is still too early to guide treatment decisions by tumor DNA sequencing and define tumor mutations as potential targets for tumor therapy.

There are though alterations that may give us predictive information: *ESR1* mutations seem to be predictive to resistance to aromatase inhibitors. And Her-2-activating mutations show possible sensitivity to neratinib, a tyrosine kinase inhibitor normally used in Her-2 positive breast cancer (62, 63).

1.2 Blood-based analyses of cancer

1.2.1 Liquid Biopsy – Introduction

Although the treatment of breast cancer has markedly changed over the last decades, a common problem in treating patients with metastatic breast cancer is acquired resistance to systemic treatment. Treatment decisions are mainly made on basis of the tumor genotype (64). Tumor biopsy is still standard of care to receive prognostic, predictive and diagnostic information. Tumor tissue often provides only a snapshot of tumor information and is not able to picture its heterogeneity or dynamic adaptations caused by anticancer drugs (65). Multi-site testing at different time points is not feasible due to possible complications of tumor biopsies as well as its influence on patients' quality of life. Hence, treatment decisions often depend on the result of one single tumor biopsy. That is why other methods for representation of disease biology are getting more important. The biggest challenge in treatment of cancer patients is tumor heterogeneity resulting in acquisition of resistance and tumor progression. Sometimes even much earlier before clinical symptoms or radiologic progression come up. New biomarkers such as various activating mutations in cancer types have led to the development of targeted therapies but there is still a lack of effective therapies against most genomic aberrations (64).

As a diagnostic biomarker liquid biopsy plays an important role in early detection of cancer as well as in monitoring of minimal residual disease. Its predictive approach includes assessment of molecular heterogeneity of overall disease, monitoring of tumor dynamics at different points of time during a treatment course, identification of genetic determinants for targeted therapy, the evaluation of early treatment response as well as assessment of evolution of resistance. Liquid biopsy as a prognostic biomarker may help identifying patients with high risk of recurrence (65).

Blood provides several types of cancer-derived materials such as nucleic acids including DNA, cell-free DNA (cfDNA) and circulating tumor DNA (ctDNA), microRNAs, non-coding RNA, and microvesicles as a result of their release in the circulation or even their spread as circulating tumor cells (CTCs) or clusters (65, 66). For the use of liquid biopsies in clinical care there are three criteria a tumor biomarker test must meet which have been defined by the Evaluation of Genomic Applications in Practice and Prevention Initiative (EGAPP): analytical validity, clinical

validity and clinical utility (67). Analytical validity includes examining reliability, reproducibility and correctness of the test. The clinical validity of a test requires its capability to divide a population into separate groups with different clinical outcomes. For the clinical utility there needs to be proof that outcomes for the tested patients differ from those who were not tested (66, 67).

1.2.2 Circulating tumor cells (CTCs)

Circulating tumor cells detected in the blood stream originate from tumor deposits. There are different possible mechanisms for the intravasation of tumor cells including active and passive ways. Most of them seem to persist only a short time having a half-life of less than 3 hours and cannot be detected anymore after surgical resection. Others live longer in the blood stream and have the potential to give rise to metastases from primary or other lesions in distant organs (68). According to their morphology they are heterogeneous and some of them even circulate in clusters in a range between two CTCs caught in mitosis to large microemboli with > 50 cells in the peripheral vasculature (69).

In metastatic breast cancer the presence of CTCs is associated with short survival. Cristofanilli et al showed that patients with levels of CTCs equal to or higher than 5 per 7.5ml of whole blood had a shorter median progression-free survival and overall survival to patients with fewer than 5 CTCs per 7.5ml. At the first follow-up visit after initiation of a new therapy, this difference between the groups persisted. The CTC levels gave an estimate of disease progression and survival earlier than by traditional imaging methods (70).

Most of the patients with metastatic cancer have fewer than 10 cells per ml which makes it more complicated to isolate them. There are many different isolation techniques to sort, purify and identify CTCs without losing or damaging them. These strategies depend on physical properties of tumor cells, their expression of unique cell surface markers and the effective depletion of normal leukocytes to reveal untagged CTCs. Because of their rarity the enrichment of CTCs before detection is indicated (69).

1.2.2.1 Isolation of CTCs

Filtering technologies are a simple way of measurement of CTCs because many epithelial cells are often larger than leukocytes (71). Due to great variations in the size of CTCs their measurement can be challenging. Other isolation techniques are based on biological or physical properties that distinguish CTCs from normal cells of the blood including density, electrical charge, secretion of marker proteins or the invasion of CTCs through collagen-coated surfaces (72-74).

Affinity based enrichment is commonly used for separation of CTCs from blood cells. These technologies take advantage of different antigen expressions of CTCs and blood cells. One example is the epithelial cell surface marker EpCAM, which can be detected by the commercial FDA-cleared technology CellSearch (75-77). A CTC based on CellSearch is defined as any EpCAM positive, intact cell with a minimum size of 4µm, CK+/CD45-, with a nucleus that is at least 50% inside the cytoplasm (78). Blood cells are first fixed and then exposed to antibody. Afterwards they have to be separated by the application of a magnetic field. It represents a reproducible and effective method but it is associated with a relatively small number of recovered CTCs. Notably CTCs that have undergone epithelial-to-mesenchymal transition and are often associated with chemoresistance cannot be detected by EpCAM – dependent technologies (79, 80).

Therefore, depletion of leucocytes from a blood sample is a promising alternative strategy because leucocyte cell surface markers are well characterized and invariant. With help of a modern microfluidic technology, nucleated cells are separated from red blood cells, platelets and plasma and then arrayed within a single file. This magnetic deflection of inertially focused tagged leucocytes is very efficient (81, 82).

1.2.2.2 CTCs as a prognostic marker

The prognostic value of detected CTCs by CellSearch has been shown in several trials on metastatic breast, prostate and colon cancer (69, 70, 83). However, it is not only the presence of CTCs but also their change during tumor therapy that is associated with patient survival (84-86).

The SWOG S0500 trial hypothesized that patients with metastatic breast cancer who show five or more CTCs per 7.5ml whole blood but for whom chemotherapy has failed to reduce CTCs to less than five per 7.5ml whole blood by first follow-up after starting a new first-line chemotherapy might have a benefit from an early change to another chemotherapy regimen. 624 patients were enrolled into the study. After the first follow-up 57% of patients with increased CTCs at baseline had CTC levels that were no longer increased. 43% that still had increased CTCs were randomly assigned to continue initial therapy or switch to alternative therapy. There was no difference in either PFS or OS. The prognosis for patients without increased CTCs at baseline, with increased CTCs at baseline but not at first follow-up and for those with persistent increased CTCs were significantly different overall. This strategy did not improve patients' outcome but validates other studies that showed a worse prognosis in association with persistent increased CTCs after chemotherapy (86, 87).

The association between CTC changes and improved survival was also evaluated in a phase III trial of metastatic prostate cancer patients receiving abiraterone versus placebo. Here CTC

enumeration by CellSearch and other parameters after 12 weeks of treatment were significantly associated with reduced survival (88). The role of CTC elimination as an early signal of drug activity was also part of the Treat CTC-trial. In light of retrospective data suggesting a benefit of Her-2-directed therapy in both Her-2-overexpressing and Her-2 nonamplified breast cancer patients, it was hypothesized that women with Her-2 nonamplified tumors might benefit from trastuzumab. This phase II trial investigated whether six cycles of trastuzumab treatment decreases the detection rate of CTC in patients with primary breast cancer without Her-2-expression. Trastuzumab could not significantly decrease the CTC detection rate (89).

Most recently a large pooled analysis confirmed follow-up CTC assessments after a median of 29 days to be predictive for OS in metastatic breast cancer patients undergoing tumor-specific therapy. It could be shown that patients with persistent CTC-Negativity at baseline and the first follow-up had a prolonged OS compared to the other patients. Moreover the CTC responders, defined as the patients, who were CTC positive as baseline and negative at first follow-up did also have a significant benefit in survival compared to non-responders (90).

1.2.3 Circulating cell-free DNA (cfDNA)

Circulating, cell-free nucleic acids in the bloodstream were first described by Mandel and Métais in 1948. Its release into the bloodstream may originate from the primary tumor, tumor cells circulating in peripheral blood, metastatic deposits and normal cell types like hematopoietic and stromal cells. cfDNA can also be found in healthy subjects and is heterogenous both in size and composition (91, 92). During tumor development there is an increased accumulation of cfDNA in the blood mainly released by apoptotic and necrotic cells. This seems to be associated with a rapid increase in circulating nucleosomes, nuclear complexes of histones and DNA, during anticancer treatments and with a decrease at disease progression (93).

There are differences between apoptotic and necrotic cells depending on the size of cfDNA. Apoptotic cells produce DNA fragments of 180 – 200 base pairs, necrotic cells, on the other hand, usually release DNA fragments of 10,000 base pairs or more (94).

There are different methods for quantification of cfDNA, mainly based on fluorometry such as the Picogreen assay or ultraviolet spectrometry. The quantitative polymerase chain reaction (PCR) is even more sensitive whereas for the detection of rare mutations methods like next-generation sequencing are common.

Additionally the integrity of cfDNA seems to be informative. The ALU DNA integrity assay, which is performed in real-time qPCR, measures the amount of short and long cfDNA fragments based on noncoding repeat sequences. This led to the incorporation of the cfDNA

integrity index which differs between healthy controls and patients with primary breast cancer as well as between primary and metastatic breast cancer patients (94, 95).
cfDNA represents mainly the genome of dying cells and the benefit from cfDNA measurement leading to a clinical decision is unknown because it is not strictly cancer-specific.

1.2.4 Circulating tumor DNA (ctDNA)

In patients with cancer, a fraction of cfDNA is derived from tumor cells and also known as ctDNA. The levels of ctDNA may be influenced by different factors such as tumor burden, tumor histology, stage or accessibility to circulation. Somatic genetic alterations of cancer can be found in almost every cancer cell and therefore, mutations in ctDNA reflect the mutations of the primary tumor. These analyses of ctDNA mutations may provide information about the potential of targetable driver genes such as *KRAS, BRAF, EGFR* and *PIK3CA*. Moreover their detection may play an important role in monitoring their levels under therapy and may reflect residual cancer (96). The levels of ctDNA have been shown to correlate with tumor burden and response to tumor therapy. The amount of tumor-specific DNA varies from < 1% to > 90% making the analysis of ctDNA a challenging field (97).
There are targeted and untargeted approaches available for the analysis of plasma DNA. For targeted approaches “a priori” knowledge of investigated genetic changes from the primary tumor is needed and may have implications for therapy decisions. An untargeted approach, without knowing specific genetic changes, includes genome-wide analysis of ctDNA and may be used for identification of new therapeutic targets or detection of molecular resistance, but also determination of the overall amount of ctDNA.

1.2.4.1 Technologies for ctDNA analysis

There are several preanalytical factors which may have an influence on the quality of ctDNA analysis. For the isolation of cfDNA, 5 to 10ml whole blood are collected in Ethylenediaminetetraacetic acid (EDTA) tubes representing a suitable choice for stability and quality of cfDNA. In the next step plasma is separated by centrifugation. Plasma should be preferred over serum and processed immediately after blood collection due to cell lysis of normal blood cells which may have an impact on ctDNA levels. The extraction of ctDNA from plasma is done by using commercially available kits. After isolation of ctDNA, somatic genomic aberrations can be detected using specific assays (78).

1.2.4.1.1 Targeted approaches

The analysis of known specific changes in plasma and serum started with the identification of somatic point mutations in cfDNA in 1994 (98). Since then a variety of new technologies have been developed. PCR-based liquid biopsy technologies have become more sensitive over the last years in order to enable the detection of point mutations at low allele fractions.
The most common method of digital PCR is the droplet digital PCR. Amplification of each DNA template is done in single emulsion droplets. Here reactions are partitioned into nanoliter-sized droplets which allows rapid analysis of thousands of droplets per sample through a microfluidic system (95, 99, 100).

An alternative method “Beads, Emulsion, Amplification, Magnetics digital PCR” (BEAMing) provides a combination between emulsion PCR with magnetic beads and flow cytometry. Each droplet contains a bead with thousands of copies of the single DNA molecule. The analysis through flow cytometry or optical scanning instruments can help to determine the fraction of mutated DNA (101). At the moment there are several other high-sensitivity PCR assays for ctDNA analysis available including real-time quantitative PCR-based (RT Q-PCR) techniques such as Intplex Q-PCR, the amplification-refractory mutation system (ARMS) or the co-amplification at lower denaturation temperature (COLD-PCR) (65). Furthermore epigenetic alterations such as promoter/enhancers methylation can be measured through ctDNA. Methylation-specific PCR, for instance, is a common technique for gene-specific detection of DNA methylation (102).

Another method and example for targeted deep-sequencing is a hybrid technique containing Next generation Sequencing (NGS) and a combination of PCR and NGS in order to identify specific genomic regions. Synchronous coefficient of drag alteration (SCODA), for instance, enriches the mutant alleles and subsequently analyzes them by NGS (103). Other methods are the tagged-amplicon sequencing (Tam-Seq) (104), which identifies rare cancer mutations at an allele frequency as low as 2% or the Safe Sequencing System (SafeSeqS). This approach uses single molecule barcoding before PCR amplification and is able to detect single somatic mutations on ctDNA (105).

1.2.4.1.1.1 Untargeted approaches – whole-genome sequencing

Genome-wide analysis is independent from recurrent genetic changes and therefore useful for all patients. Whole Genome Sequencing (WGS) and Whole Exome Sequencing (WES) are

technologies used to characterize somatic chromosomal aberrations and copy number variations. There are two genome-wide methods being applicable to liquid biopsy.
Personalized Analysis of Rearranged Ends (PARE) identifies translocations and other somatic rearrangements using a next-generation mate-paired analysis (106). Digital karyotyping is a genome-wide technique to detect copy number variations and novel sequences giving more insight into intratumoral heterogeneity (107).
Notably, due to limited analytical sensitivity, untargeted approaches can only be used in cases in which tumor-derived DNA accounts for more than 3-10% of the total circulating cell-free DNA (cfDNA).

1.2.4.2 Clinical utility

1.2.4.2.1 Tumor genotyping

One advantage and a promising field of ctDNA utility is the assessment of a genomic profile in the advanced setting of breast cancer. While activating mutations such as *PIK3CA* are more common and represent a target for tumor-specific therapy, other mutations are rare and can be acquired in metastatic setting. Therefore primary tumor tissue is often not representative because it does not reflect the current mutational status.
Identifying specific genomic alterations to guide mutation-targeted therapies was done in non-small lung cancer when EGFR mutations and EML-ALK4 rearrangements were detected. Moreover BRAF mutations in melanoma, KRAS mutations in colorectal cancer and Her-2 amplification or PIK3CA mutations in breast cancer represent therapeutical targets when effective therapies are available (69, 78).
ESR1 mutations occur in about 30% of metastatic breast cancer and are associated with resistance to endocrine therapy in HR positive disease (108, 109). The most effective treatment of *ESR1* mutated breast cancer is currently unclear, showing resistance to subsequent therapy with aromatase inhibitors and low sensitivity to fulvestrant (110, 111). The SoFEA trial showed no difference in PFS or OS in AI-pretreated patients receiving AI, fulvestrant or fulvestrant plus AI (112). However, a prospective-retrospective analysis on samples of the SoFEA and PALOMA-3 trial showed that *ESR1* mutations in plasma DNA predicted relative resistance to AI and relative sensitivity to fulvestrant. The combination of fulvestrant and a CDK4/6-inhibitor appeared to be effective in both patients with or without *ESR1* mutations (36, 112, 113).
A secondary analysis of the BOLERO-2 trial, when cfDNA was evaluable for *ESR1* from 541 patients, showed a poor prognostic association on OS and more aggressive behavior (114).

When analyzing plasma samples of the PALOMA-3 trial, when patients with HR positive breast cancer received palbociclib and fulvestrant, O'Leary et al showed that a change of *PIK3CA* ctDNA after 15 days of treatment was predictive for PFS. While there have been no predictive biomarkers for CDK4/6-inhibition yet, early ctDNA dynamics may have a potential (115).
The multicohort, prospective phase 2 platform trial plasmaMATCH aimed to assess accuracy and ability of ctDNA testing to detect and treat targetable mutations in metastatic breast cancer patients. Potentially targetable mutations were *ESR1, AKT1, HER2* or *PTEN.* According to these mutations, patients were enrolled in four different treatment arms matched to mutations. A fifth cohort recruited patients with TNBC and no targetable mutation, receiving olaparib plus an ATR inhibitor and results have not been published yet.
For ctDNA analysis digital droplet PCR was done in all patients. After recruitment of 680 patients an error-corrected targeted sequencing for a panel of 73 genes was also accomplished. *PIK3CA* ctDNA testing was performed additionally but due to ongoing phase 3 trials investigating the treatment of *PIK3CA* mutated breast cancers, there was no extra therapeutic cohort planned. Patients harboring an ESR1 mutation were enrolled in treatment cohort A and received fulvestrant, Her2-mutated patients received neratinib alone or in combination with fulvestrant when HR positive in cohort B, patients with an AKT1 mutation and HR positive breast cancer received the AKT-inhibitor capivasertib plus fulvestrant and cohort D included patients with an AKT pathway activating mutation and HR negative tumors. The primary endpoint of this study was confirmed objective response rate.
Mutations were found in 50.1% of 1044 patients, while targetable mutations for enrollment in one of the treatment cohorts were detected in 34.5%. In cohort A 8% of the patients had a partial response with a median duration of response of 7 months; in cohort B, a response to therapy was confirmed in 25% with a median PFS of 5.4 months; 22% patients with an AKT mutation in HR positive breast cancer in cohort C had a partial response and a clinical benefit rate of 39%; in cohort D, 11% had a confirmed partial response and a median PFS of 3.9 months. There was a high agreement between the ctDNA testing technologies with high sensitivity for identified mutations. Moreover accuracy and availability of ctDNA were comparable with tissue-based mutation testing and ctDNA testing results were found in 99% of the patients. This study showed that ctDNA testing with the used assays can be implemented in clinical routine and identify patients with common and rare targetable mutations (116).

1.2.4.2.2 Detection of early relapse

While adjuvant chemotherapy or endocrine therapy is aimed to reduce the risk of recurrence in breast cancer patients, ctDNA might have an impact on detecting micrometastatic disease.

A prospective analysis of 55 patients undergoing neoadjuvant chemotherapy in early breast cancer showed an association between detected ctDNA after surgery or at follow-up and metastatic relapse. Increased ctDNA levels were also predictive for worse prognosis (117). Low ctDNA levels in early breast cancer can be challenging in technical aspects. The CancerSEEK multi-analyte blood test, for instance, combines the evaluation of genetic alterations in ctDNA and protein biomarkers providing a high specificity and concordance between tumor tissue and ctDNA (65, 118). The test was performed in over 1000 patients with one of eight non-metastatic cancer types including ovarian, liver, stomach, pancreatic, colorectal, lung, esophageal and breast cancer. The test was highly sensitive for ovarian cancer but associated with less sensitivity in other cancers and low sensitivity in stage I cancers, furthermore providing a high false-positive rate of around 50% (119).

1.2.4.2.3 Treatment response monitoring in metastatic setting

Due to the association of ctDNA levels and tumor mass, ctDNA as a monitoring tool under treatment in metastatic breast cancer patients is of great interest reflecting intratumoral heterogeneity and clonal evolution.

A prospective single-center study compared the sensitivity of measuring ctDNA and other circulating biomarkers for monitoring of tumor burden in 30 patients with metastatic breast cancer. For analysis tagged-amplicon deep sequencing for *PIK3CA* and *TP53* or paired-end whole genome sequencing was used. Additionally, measures of CA 15-3 levels and counting of circulating tumor cells was assessed. Serial blood samples were taken at an interval of 3 weeks or more. ctDNA showed superior sensitivity to that of other circulating biomarkers and its change correlated with change in tumor burden. Higher ctDNA levels and circulating tumor cells had prognostic significance and were associated with worse OS, while CA 15-3 was not prognostic (120).

1.3 Aim of the dissertation

Based on the current knowledge of liquid biopsy methods in various cancer types, we wanted to investigate its potential role in a cohort of metastatic breast cancer patients treated at the Division of Oncology at the Medical University of Graz.

In the first part of the dissertation, the focus lies on the prognostic role of an untargeted method named mFAST-SeqS and its applicability as a monitoring tool for treatment response. Blood-based parameters such as cancer antigen (CA) 15-3 or carcinoembryonic antigen (CEA) are commonly used in patients undergoing systemic therapy for response monitoring, but they are associated with less sensitivity or specificity. Several studies showed the prognostic and predictive value of CTCs, cfDNA or ctDNA in several solid malignant tumors (121-129). For this reason we tested the capability of CTCs and ctDNA employing mFAST-SeqS compared to CEA and CA 15-3 as a monitoring tool in patients under tumor-specific therapy.

In the second project the focus was on a specific alteration in patients with metastatic HR positive breast cancer and its prognostic role. Around 40% of these patients harbor a *PIK3CA* mutation, which can be targeted by the PI3K inhibitor alpelisib. In the SOLAR-1 trial, this treatment led to an improvement in PFS (51). The detection of PIK3CA mutations can be performed by liquid biopsy or tissue testing. Due to the importance of PIK3CA testing project 2 was aiming at comparing the two methods in an extended cohort of HR positive metastatic breast cancer patients treated at the Division of Oncology at the Medical University of Graz, and evaluating whether liquid biopsy based detection of *PIK3CA* mutations can be further improved by mFAST-SeqS based detection of ctDNA fraction.

2 Materials and Methods

2.1 Project 1

This section was similarly published in Suppan et al. (130).

2.1.1 Patient data and blood samples

We included 29 female patients with metastatic HR-positive, Her-2 negative breast cancer between June 2014 and December 2016 treated at the Division of Oncology, Department of Internal Medicine, Medical University of Graz, Austria. These patients were planned for antihormonal treatment in combination with a CDK 4/6 inhibitor. This study was approved by the ethics committee of the Medical University Graz (ethical approval numbers 24-539 ex

11/12 and 21-227 ex 09/10*).* An informed consent was signed by all patients. All experiments were carried out in consideration of the guidelines for good scientific practice as officially required from the Medical University of Graz. Patient data including baseline characteristics and histological features was documented. Blood samples were taken at different points of time: before starting first-line tumor-specific therapy, at week 2 – 4 of treatment, at time of CT scan (week 8 – 12) and at the beginning of a new treatment line due to progressive disease. Baseline was defined as time of study enrollment. Extent of disease and response during the treatment course was determined by the use of conventional radiological staging methods.

2.1.2 Preparation of plasma DNA

0.225 ml of a 10% neutral buffered solution containing formaldehyde (4% weight per volume, Sigma-Aldrich, Vienna, Austria) was added after blood collection in EDTA vacutainer tubes (BD Biosciences, Heidelberg, Germany). Plasma was separated by centrifugation at 200g for 10 minutes. This process was followed by 1600g for 10 minutes with brake and acceleration powers set to zero. The supernatant was discarded after centrifugation and centrifuged again at 1600g for an additional period of another 10 minutes. Storage of plasma was done at -70°C, in 2 ml tubes. We used the QIAamp Circulating Nucleic Acid Kit (Qiagen, Hilden, Germany) for preparation of plasma DNA, and proceeded accordingly to the manufacturer's recommendations. For quantification we used the Qubit dsDNA HS Assay Kit (Life Technologies, Vienna, Austria).

2.1.3 Modified Fast Aneuploid Screening Test-Sequencing System (mFAST-SeqS)

Temporarily 0.5 - 2 ng of plasma DNA was amplified with Phusion Hot Start II Polymerase in 5 PCR cycles while using target-specific L1 primers. For the second PCR we added Illumina specific adaptors: after purification of the PCR products with AMPure Beads (Beckman Coulter, Brea, CA, USA) we directly used 10µl. L1 amplicon libraries were sequenced on an Illumina MiSeq generating 150bp single reads. The aim was to at least acquire 100.000 reads. For better interpretation of LINE1-sequences we compared read counts of each chromosome arm to a control population (n=18) using z-score statistics (131). The result is a genomewide z-score representing the tumor fraction.

2.1.4 Genome-wide copy number profiling

We used the TruSeq DNA LT Sample preparation Kit (Illumina, San Diego, CA, USA) to prepare shotgun libraries from 5-10 ng of plasma DNA. Because of the fragmentation of plasma DNA, the fragmentation step was kept off and up to 25 PCR cycles were performed. These libraries were sequenced on Illumina MiSeq or NextSeq (Illumina, San Diego, CA, USA), sequencing data was established with our optimized in-house plasma-Seq script (132, 133). In addition data was analyzed with an ichorCNA algorithm in order to calculate tumor fraction from ultra-low-pass whole-genome sequencing (ULP-WGS) (134).

2.1.5 Enumeration of CTC

7.5 ml of whole blood was drawn into CellSave tubes (Veridex LLC, Janssen Diagnostics, Rarities, NJ, USA) for CTC enrichment. A size-based microfilter device (71, 135) has been used for CTC capture. First, blood samples were diluted 1:1 with 1x phosphate-buffered saline (PBS), then fixed for 10 minutes with 1% formalin (Sigma-Aldrich, Vienna, Austria). Fixation was followed by processing blood through a microfilter. This was done at a constant flow rate of 75 ml/hour while using a motorized syringe pump. Double immunofluorescence staining was used for CTC identification and enumeration: explicitly pan-cytokeratin (pan-CK) and CD45 antibody. First filters with captured CTCs were placed on a glass microscope slide. They were blocked for 30 minutes with blocking buffer containing 5% normal goat serum (Life Technologies) and 3% Triton X-100 (Sigma Aldrich) at room temperature. In a next step samples were incubated with primary antibodies (Anti-CD45 (DAKO, Glostrup, Denmark) and polyclonal rabbit anti-cytokeratin (1:300; DAKO)), and consequently secondary antibodies (Goat anti-mouse Alexa 594 and goat anti-rabbit Alexa 488 (both 1:100, Life Technologies), again at room temperature. Each for a period of time of one hour.

In the final step all samples were counterstained with four 6-diamidino-2-phenylindole (DAPI, Invitrogen). All samples were mounted on coverslips with ProLong Gold Antifade mounting media (Life Technologies). The entire microfilter surface was screened in order to identify CTCs using a confocal laser-scanning microscope (Zeiss, Oberkochen, Germany). A positive CTC was defined as a CKpositive/CD45 negative nucleated cell on the filter.

2.1.6 Statistical analysis

GraphPad Prism 6.0 (GraphPad Software, San Diego, CA, USA) and SPSS 23 (SPSS, Inc., Chicago, IL, USA) were used for statistical analyses and plotting of data. The continuous variables were reported as medians (25^{th}-75^{th} percentile). The categorical variables were summarized as absolute frequencies and percentages. The chi-square test (expected cell counts ≥5) or Fisher's exact test (expected cell counts <5), was used for analyzing associations between categorical variables. A linear mixed effect model was used for serial z-score measurements (n=108). In order to account for the unbalanced z-score data it was combined with a random-intercept at patient level. It was also obtained for the clustered nature of z-score measurements within individual patients. For the random effects an independent variance-covariance structure was assumed. Nonparametric Spearman correlation was used for correlation analysis of baseline markers. In order to estimate the median follow-up time we used the reverse Kaplan-Meier method (136). The time of blood sampling to the patients' deaths from any cause was defined as overall survival (OS). The time of first blood sampling until the date of clinical progression or death was the progression-free survival (PFS). The censoring date was the last day of follow-up if one of these events was not observed. A log-rank test was used for analyzing differences in survival curves. Cox Proportional-Hazards regression was used for performing multivariate survival analysis. Furthermore, all p values were two-sided. When p values were <0.05 they were considered statistically significant.

2.2 Project 2

This section is part of a work that has been submitted for publication.

2.2.1 Patients and sample collections

We included 70 locally advanced or metastatic breast cancer patients between February 2017 and September 2020, treated at the Division of Oncology, Department of Internal Medicine, Medical University of Graz, Austria. One patient who had received a bone marrow transplantation was excluded from the study. The study was approved by the ethics committee of the Medical University Graz (ethical approval number 21-227 ex 09/10). All patients signed an informed consent. All analyses were carried out in consideration of the guidelines for good scientific practice as officially required from the Medical University of Graz. Documentation and collection of patient data was done in an electronic database system. Again, blood sampling was performed at different points of time: before initiation of tumor-specific therapy, during the treatment, and/or when initiating a new treatment line due to progressive disease.

The most recent tissue from a metastatic biopsy or the primary tumor was used for tissue analyses.

2.2.2 High-resolution screening for PIK3CA mutations in plasma

To screen for *PIK3CA* mutation, the SiMSen-Seq method (simple, multiplexed, PCR-based barcoding of DNA for sensitive mutation detection using sequencing) was used (137). This technology is based on molecular barcoding of individual DNA template strands to track all sequencing reads back to a single original template and correct for PCR errors during library preparation. To assess the most common hotspots (n=11), three assays covering exons 7, 9, and 20 were designed and validated as described in (137) (Table 1).

According to the guidelines from the SiMSen-Seq inventors, three target primer pairs were designed for each exon, considering product size, primer size, annealing temperature, and complementarity. Using quantitative real-time PCR (qPCR), all primers were initially tested with a high-quality control DNA (Promega, Wisconsin, USA) and compared to a control assay. Assays with the cycle of quantification (Cq) values closest to the control assay were further evaluated after adding the barcoded hairpin primer sequences. For each exon, the best performing assay, which met all quality criteria, was chosen (Table 2). The three assays were pooled to one multiplex assay with a final concentration of 1µM using 50ng of a control DNA (Promega, Wisconsin, USA) and re-evaluated in a short depth sequencing runs until a balanced coverage of the three amplicons was obtained.
For the analysis of plasma samples, an average input of 26.3ng (range, 8.5-103.8ng) cfDNA per sample was used for library preparation. After purification with a 0.8-fold volume of AMPure XP Beads (Beckman Coulter, Brea, CA, USA), libraries were quantified with qPCR using the QIAseq Library Quant Assay (QIAGEN, Hilden, Germany) and sequenced on an Illumina MiSeq, or NextSeq using 150bp single end reads aiming for 10 million reads per sample. Barcoded SiMSen-Seq data was analyzed using Debarcer (137). After consensus read generation, we obtained an average coverage of 2185x (range 49-17227x) for all interrogated positions. The presence of mutations was reported as variant allele frequency (VAF, percentage of alternate reads relative to the total number of reads at a given position).
To evaluate the assay's sensitivity, we used the SeraCare reference material, which included the H1047R *PIK3CA* mutation at various VAFs. Error correction enabled a significant reduction of the sequencing background (Figure 1A) and a mutation detection down to a VAF of 0.125% (Figure 1B). The observed VAFs were positively correlated (r=0.9539) with reported VAFs from SeraCare assessed with ddPCR (Figure 1C, Figure 2). To determine the assay's specificity, we additionally analyzed high molecular weight DNA from five controls and five cfDNA samples from healthy individuals in duplicates. Considering only barcode families

containing a minimum of 5 reads, an average consensus read depth of 10539x (range, 3486 -18749) and 344x (range, 49-790) was obtained. One mutated consensus read at a single position could be observed in five samples of the cfDNA and four samples of the gDNA. Only one gDNA sample showed two false-positive consensus reads. Taken together, this resulted in a maximum background VAF of 0.06% for cfDNA and 0.001% for gDNA. Based on these data and to ensure a reliable and stringent variant calling, we set the LOD at a VAF of 0.25%.

Table 1. PIK3CA mutations

Exon	Mutation	Base change	COSMIC ID
7	C420R	1258 T>C	757
9	E542K	1624 G>A	760
	E545A	1634 G>A	12458
	E545D	1635 A>C	765
	E454G	1634 A>G	764
	E545K	1633 G>A	763
	Q546E	1636 C>G	6147
	Q546R	1637 A>G	12459
20	H1047L	3140 A>T	776
	H104R	3140 A>G	775
	H1047Y	3139 C>T	774

Table 2. PIK3CA SiMSen-Seq assays

Primer	**Sequence**
PIK3CA_Exon 7_F	GGACACTCTTTCCCTACACGACGCTCTTCCGATCTNNNNNNNNNNNNNNATGGGAAAGAGTGTCCCTGAGCAAGAGGCTTTGGAGTATTTCATG
PIK3CA_Exon 7_R	GTGACTGGAGTTCAGACGTGTGCTCTTCCGATCTCCAATCCATTTTTGTTGTCCAGCCAC
PIK3CA_Exon 9_F	GGACACTCTTTCCCTACACGACGCTCTTCCGATCTNNNNNNNNNNNNNATGGGAAAGAGTGTCCTGACAAAGAACAGCTCAAAGCAA
PIK3CA_Exon 9_R	GTGACTGGAGTTCAGACGTGTGCTCTTCCGATCTAGCACTTACCTGTGACTCCAT
PIK3CA_Exon 20_F	GGACACTCTTTCCCTACACGACGCTCTTCCGATCTNNNNNNNNNNNNNATGGGAAAGAGTGTCCGGAAGAAAAGTGTTTTGAAATGTGT
PIK3CA_Exon 20_R	GTGACTGGAGTTCAGACGTGTGCTCTTCCGATCTCAAGTTTATATTTCCCCATGCCA

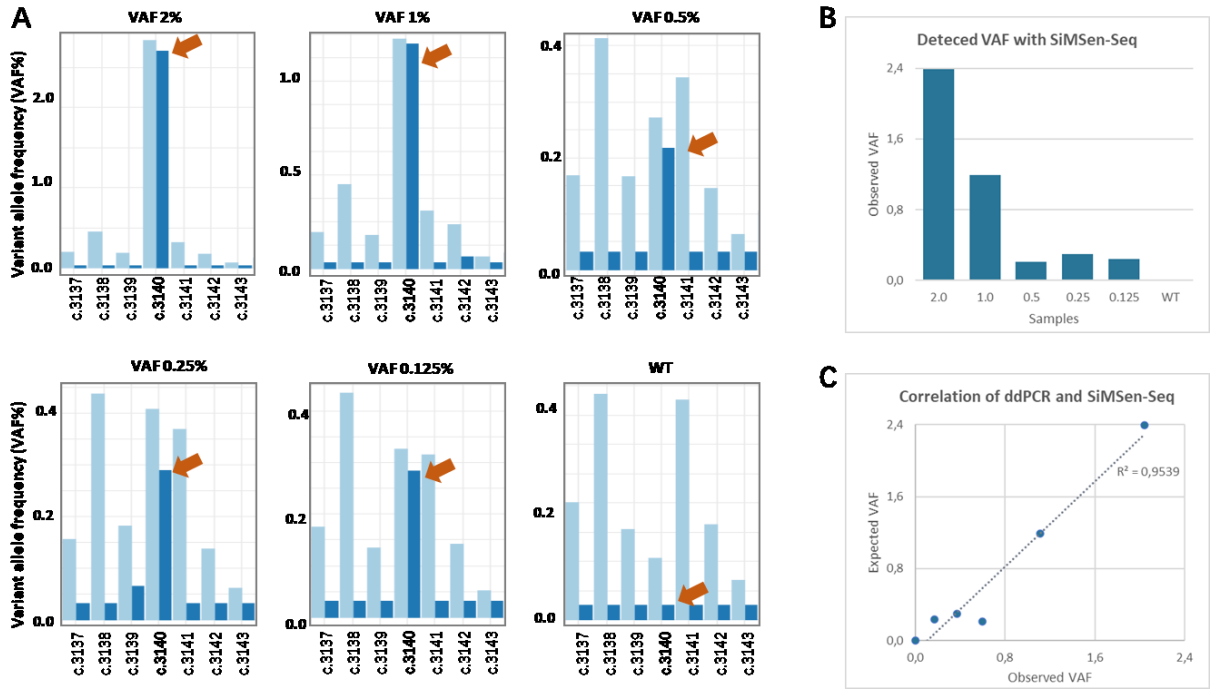

Figure 1. Representation of variant allele frequencies (VAF) of the PIK3CA hotspot mutation

Representation of variant allele frequencies (VAF) of the *PIK3CA* hotspot mutation H1047R and surrounding bases with and without error correction. (A) Shown are the VAFs of the SeraCare reference materials of the mutation c.3140A>G, p.His1047Arg (H1047R) (indicated by the orange arrow), including five bases upstream and downstream, respectively. X-axis: coding sequence-position of the *PIK3CA* gene. Y-axis: Percentage of alternate reads relative to the total number of reads at a given position. Light blue bars: raw, relative no. of alternate raw reads without UMI-based error correction. Dark blue bars: relative no. of alternate consensus reads after error correction. (B) Bar plot of observed VAF of the SeraCare reference materials (C) Linear regression of the observed versus the expected VAF

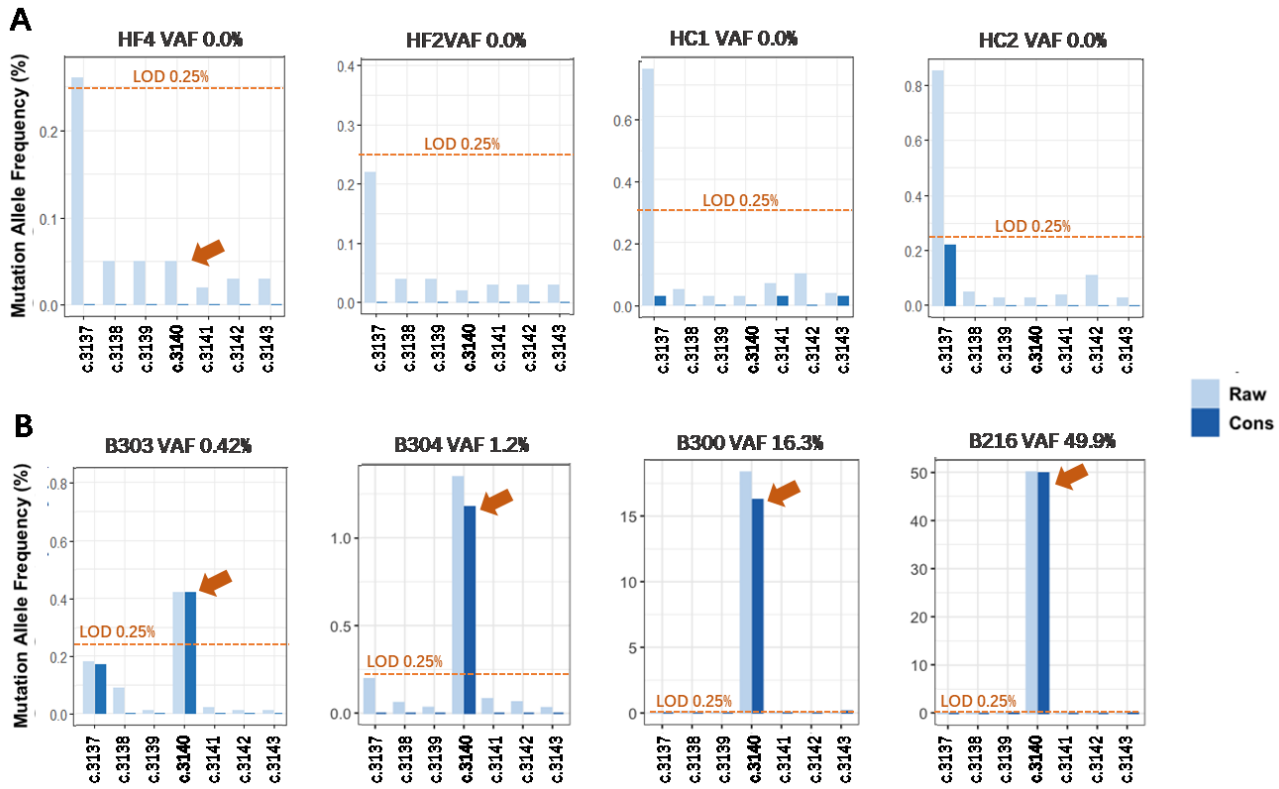

Figure 2. Representation of variant allele frequencies (VAF) of the PIK3CA hotspot mutation H1047R (indicated by the orange arrow) and surrounding bases with and without error correction. (A) Shown are the VAFs of two cfDNA (HF2 and HF4) and two genomic DNA (C1 and C2) samples, respectively, from non-cancer controls. After consensus read generation-based error correction, no false-positive reads were observed. (B) Shown are four patient samples with various levels of the *PIK3CA* mutation. While patients B320 and B304 presented low VAFs of 0.42% and 1.2%, in patients B300 and B216, the mutations were identified with VAFs of 16.3% and 49.9%, respectively. X-axis: coding sequence-position of the *PIK3CA* gene. Y-axis: percentage of alternate reads relative to the total number of reads at a given position. Light blue bars: raw, relative no. of alternate raw reads without UMI-based error correction. Dark blue bars: cans, relative no. of alternate consensus reads after error correction.

2.2.3 SiMSen-Seq library preparation of plasma DNA samples

Since a minimum of 10ng of DNA is required in a maximum of 6.35µl input material for the assay, low concentrated cfDNA samples were concentrated using the Qiagen SpeedVac system for 20 to 50 minutes at room temperature. cfDNA was added to 2µl High Fidelity Buffer (5x), 0.2µl dNTP mix (10mM), 1µl L-Carnatine (5M), 0.4µl of the *PIK3CA* multiplex assay (1µM each), 0.05µl Phusion Polymerase (2U/µl) and water to a final volume of 10µl. Samples were initially amplified with 3 PCR cycles (98°C for 10 seconds, 62°C for 6 minutes, and 72°C for 30 seconds) stating with an initial denaturation at 98°C for 30 seconds and followed by a final incubation step at 65°C for 15minutes. When the cycler achieved 65°C, protease was added to each reaction to inactivate DNA polymerase. For indexing PCR, 10µl PCR product from the first round was combined with 20µl Q5 master mix (2x), 8.4µl water, and 1.6µl universal index primer (10µM) to a final volume of 40µl. Samples were amplified at 98°C for 3 minutes, followed by 28 cycles of 98°C for 10 seconds, 80°C for 1 second, 72°C for 30 seconds, and 76°C for 30 seconds (all with ramping at 0.2°C/ second). Subsequentially, 35µl of the samples were purified using 35µl of well-vortexed AMPure XP Beads (Beckman Coulter, Brea, CA, USA) (ratio 1:1). Samples were shaken at 1600 rpm for 2 minutes, followed by an incubation step at room temperature for 5 minutes, and then placed on a magnetic stand for another 5 minutes. The supernatant was removed, and the pellet was washed twice using 200µl freshly prepared 70% ethanol and dried for 5 minutes at room temperature. Finally, samples were removed from the magnetic stand and eluted in 17.5µl of 1x TE buffer. Samples were vortexed again at 1600 rpm for 2 minutes, incubated at room temperature for 2 minutes, and were then put on a magnetic stand for another 2 minutes. Sixteen µl of the supernatant was transferred to a fresh tube and checked for quality and concentration using the Bioanalyzer High Sensitivity kit (Agilent, Santa Clara, CA, USA).

2.2.4 Tissue-based analyses

DNA was extracted from macrodissected tumor areas of unstained FFPE sections. Adequate tumor cell content was verified from HE stained parallel sections. For extraction we used the Maxwell 16 instrument (Promega, Wisconsin, USA) and the Maxwell RSC DNA FFPE Kit (Promega, CatNr: AS1450) or the Ion AmpliSeq Direct FFPE DNA Kit (Thermo Fisher Scientific, Massachusetts, USA). Quantification of DNA was done by Picogreen fluorescence, and typically, 40ng DNA was used for library preparation. NGS libraries were prepared using a custom-designed AmpliSeqHD panel covering the following mutation hotspots: *EGFR* (L858), *ERBB2* (S310, L755, V762, V777, P780), *ERBB3* (V104, E928), *KRAS* (G12, G13), *PTEN* (T319), *ESR1* (E207, K303, E380, Y537, D538), *PIK3CA* (E103, N345, C420, E542,

E545, Q546, E726, H1047, G1049), AKT1 (E17), *TP53* (R175, H179, R213, Y220, R248, R273). The panel includes all mutations evaluated in the SOLAR-1 trial (51). Molecular barcoding enables a detection threshold of 0.1% mutant allele Sequencing was performed on an Ion S5XL benchtop sequencer (Thermo Fisher Scientific) to a length of 200 base pairs. We used the open-source Ion Torrent software (Thermo Fisher Scientific, open-source, GPL, https://github.com/iontorrent/) for initial data analysis including base calling, alignment to the reference genome (hg19) using the TMAP mapper, and variant calling by a modified diBayes approach. Called variants were deconvoluted with regards to molecular barcodes and annotated using open source software ANNOVAR (138) and SnpEff (139). Further evaluation and visual inspection of all coding nonsynonymous mutations was done in IGV (http://www.broadinstitute.org/igv/). We excluded variant calls due to technical read errors or sequence effects.

2.2.5 Statistical analysis

All statistical analyses were performed with Stata 16.1 (Stata Corp., Houston, TX, USA). Continuous variables were reported as medians [25^{th}-75^{th} percentile], and count data as absolute frequencies (%). The distribution of baseline variables between patients with or without a *PIK3CA* mutation (binary variable) was assessed with rank-sum tests (continuous variables) and χ^2, or with Fisher's exact tests (categorical variables). The agreement between plasma and tissue was assessed with a kappa score and 95% CIs. In order to assess the statistical significance of differences between plasma and tissue results we used the exact McNemar's test. The correlation between z-scores and mutant *PIK3CA* allele fractions was determined by the Spearman rank correlation coefficient. In an explorative analysis, we associated *PIK3CA* mutation status with progression-free survival using Kaplan-Meier estimators, log-rank tests, and Cox proportional hazards regression.

3 Results

3.1 Project 1

This section was similarly published in Suppan et al. (130).

3.1.1 Patient characteristics

After a median follow-up time of 27 months (± 1.9) progressive disease occurred in 25 out of 29 patients (86.2%). 12 out of 29 patients died (41.4%). The most common localizations of metastases were bone in 20 (69.0%) patients, liver in 10 (34.5%) and lungs in 13 (44.8%). Treatment of patients consisted of chemotherapy, antihormonal therapy, immune therapy or combinations. Table 3 shows baseline characteristics.

Table 3. Baseline characteristics of patients (n=29) (as published in (130))

Category	Number	%
Total	29	
Age at the time of sampling (years) Median and range	 56 (50 – 68)	
Menopausal status Premenopausal Postmenopausal	 15 14	 51.7 48.3
Histologic type IDC/NST ILC Mixed type Other	 25 2 1 1	 86.2 6.9 3.4 3.4
Tumor grading (at primary diagnosis) G1 G2 G3 Unknown	 0 12 16 1	 0 41.4 55.2 3.4
Tumor size (primary tumor) pT1 pT2 pT3/pT4 Unknown	 10 9 4 6	 34.5 31 13.8 20.7
Lymph node status N0 N1-3 Unknown	 10 12 7	 34.5 41.4 24.1
ER status Negative Positive	 5 24	 17.2 82.8
PR status Negative	 9	 31

Positive	20	69
Her2 status		
Negative	21	72.4
Positive	8	27.6
Subtype (primary tumor)		
HR+/Her2 –	18	62.1
HR-/Her2-	3	10.3
Her2+	8	27.6
Bone metastases		
No	9	31
Yes	20	69
Lung metastases		
No	16	55.2
Yes	13	44.8
Liver metastases		
No	19	65.5
Yes	10	34.5
Other metastases		
No	7	24.1
Yes	22	75.9
Number of metastatic sites		
One	9	31
Multiple	20	69
Number of previous therapy lines for metastatic disease		
0	18	62.1
1	4	13.8
>= 2	7	24.1
OS status		
Alive	19	65.5
Dead	10	34.5
PFS status		
No progress	6	20.7
Progress	23	79.3
CTC >= 1		
No	12	41.4
Yes	17	58.6
CTC >= 5		
No	21	72.4
Yes	8	27.6
Z-score >= 3		
No	18	65.5
Yes	10	34.5
CTC (>= 1) or z-score (>= 3) positive		
No	10	34.5
Yes	19	65.5

IDC/NST invasive ductal carcinoma/no specific type, ILC invasive lobular carcinoma, ER estrogen receptor, PR progesterone receptor

3.1.2 Untargeted assessment of tumor fraction

We detected ctDNA in 127 serial blood samples, while CTCs were found in 97 samples. In all, there were 97 blood samples available from 29 patients providing both ctDNA and CTCs for comparison. CEA and CA 15-3 were found in 112 samples.

In 72 selected samples with a wide range of z-scores (n=39) we used the ichorCNA algorithm in order to estimate the fraction of tumor-derived fragments in cfDNA of ULP-WGS (134). In 33 patients with z-scores < 3 providing low tumor fractions we did not find informative results. There was a high correlation between ichorCNA and mFAST-SeqS for the entire cohort (n=72, R^2=*0.5666*, Spearman correlation r=0.8488, p<0.001) (Figure 3A). Interestingly enough we uncovered a subset of samples with high tumor fractions according to ichorCNA that at the same time only showed moderately elevated z-scores (Figure 3A). In these samples SCNAs only involved a few chromosome arms and were derived mostly from patient B5 (Figure 3B). In cases like that, there may be an underestimation of the true ctDNA level by mFAST-SeqS. This is because the genome-wide mFAST-SeqS z-score is calculated from all chromosome-arm specific z-scores. When we dropped these samples from the analysis, there was a close correlation again between mFAST-SeqS z-scores and the ichorCNA estimations (n=61, R^2=*0.8299*, r=0.8192, p<0.001) (Figure 3C). As SCNAs do not change much from one analysis to the other (Figure 4) we projected this correlation being even higher for samples from individual patients. And indeed, this was the case (Figure 3D and Figure 5) which suggested that mFAST-SeqS z-scores may be perfectly suited for disease monitoring.

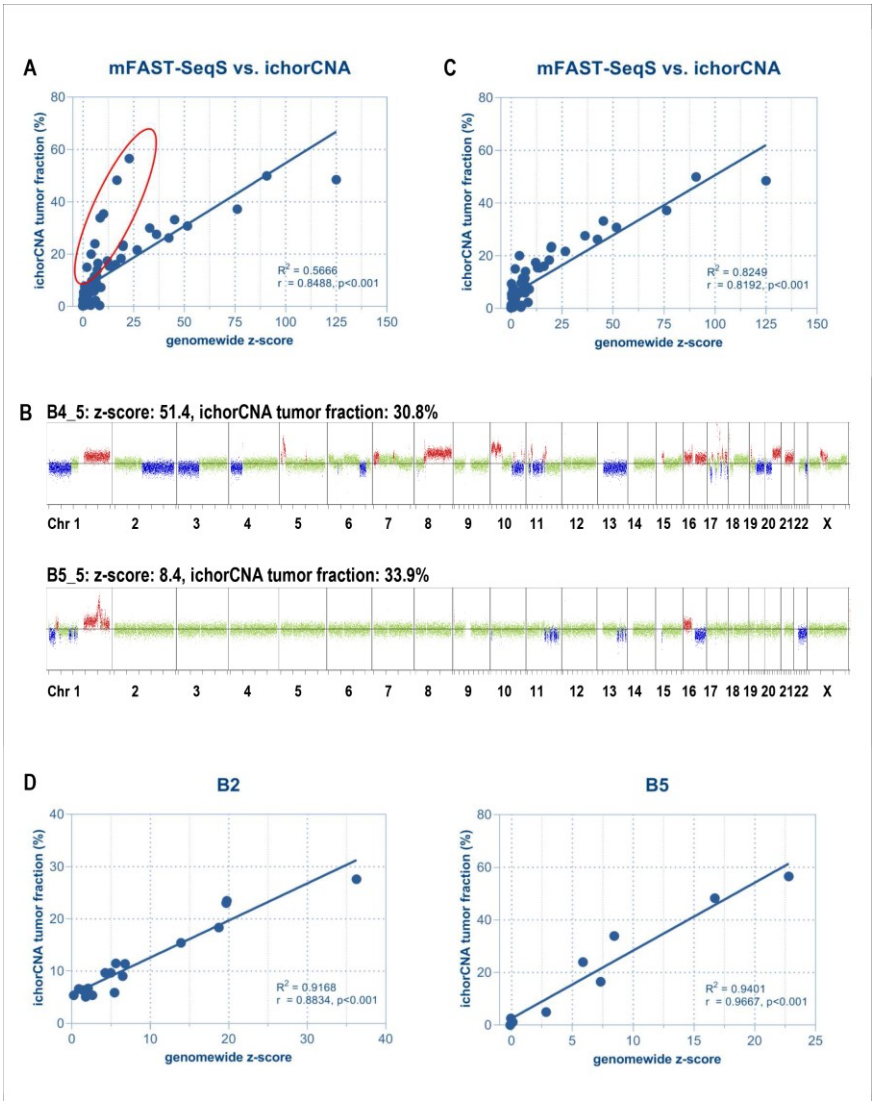

Figure 3. Correlation between mFast-SeqS based z-scores and ichorCNA tumor fractions (as published in (130))

(A) High correlation between z-score and tumor fraction (except from some samples that are highlighted in red). Most of these outliers were acquired from patient B5. (B) In samples with high tumor fraction and lower z-scores, we detected less CNAs in comparison to other samples as exemplified by two genome-wide copy number profiles. Both samples had a tumor fraction of approximately 30% based on ichorCNA. In B5, there was a low z-score of 8.4 because of the low abundance of CNAs while B4 had a z-score of 51.4 providing numerous CNAs across the genome. Green depicts balanced regions, blue indicates a loss of chromosomal material and red indicates a gain of chromosomal material. (C) What significantly improved the correlation was the removal of samples with low overall amounts of CNA. (D) In selected individual patients there was a correlation between mFAST-SeqS z-scores and ichorCNA-based tumor fractions.

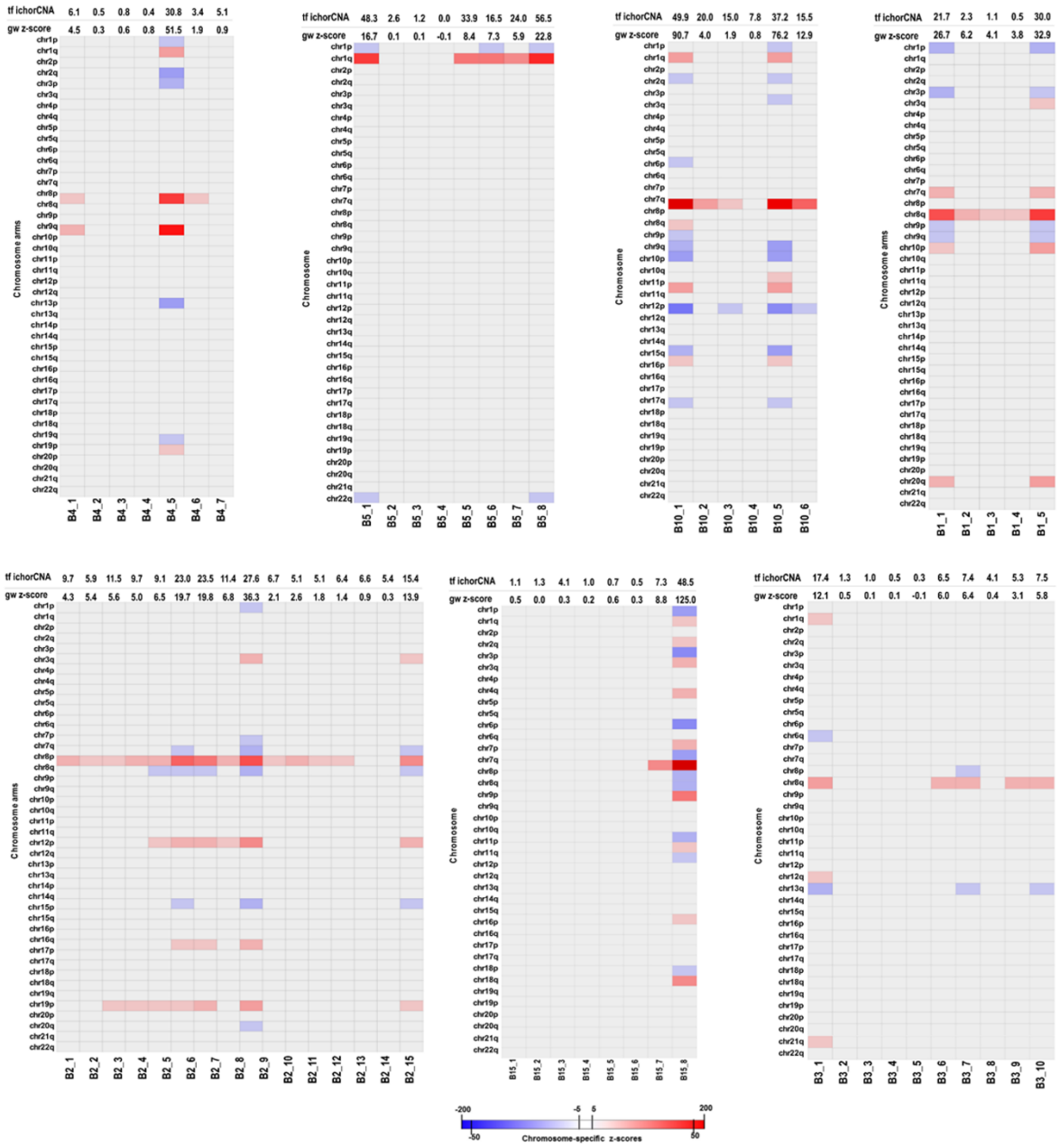

Figure 4. Plasma samples of seven patients (as published in (130))

What they show is that chromosome-arm specific CNAs are highly consistent within the same patient. Blue bars: Chromosome-specific z-scores <3. Red bars: chromosome-specific z-scores >3.

Chr, chromosome. Genomewide (gw) z-scores and tumor fraction (tf) assessed with ichorCNA are shown above the heat map.

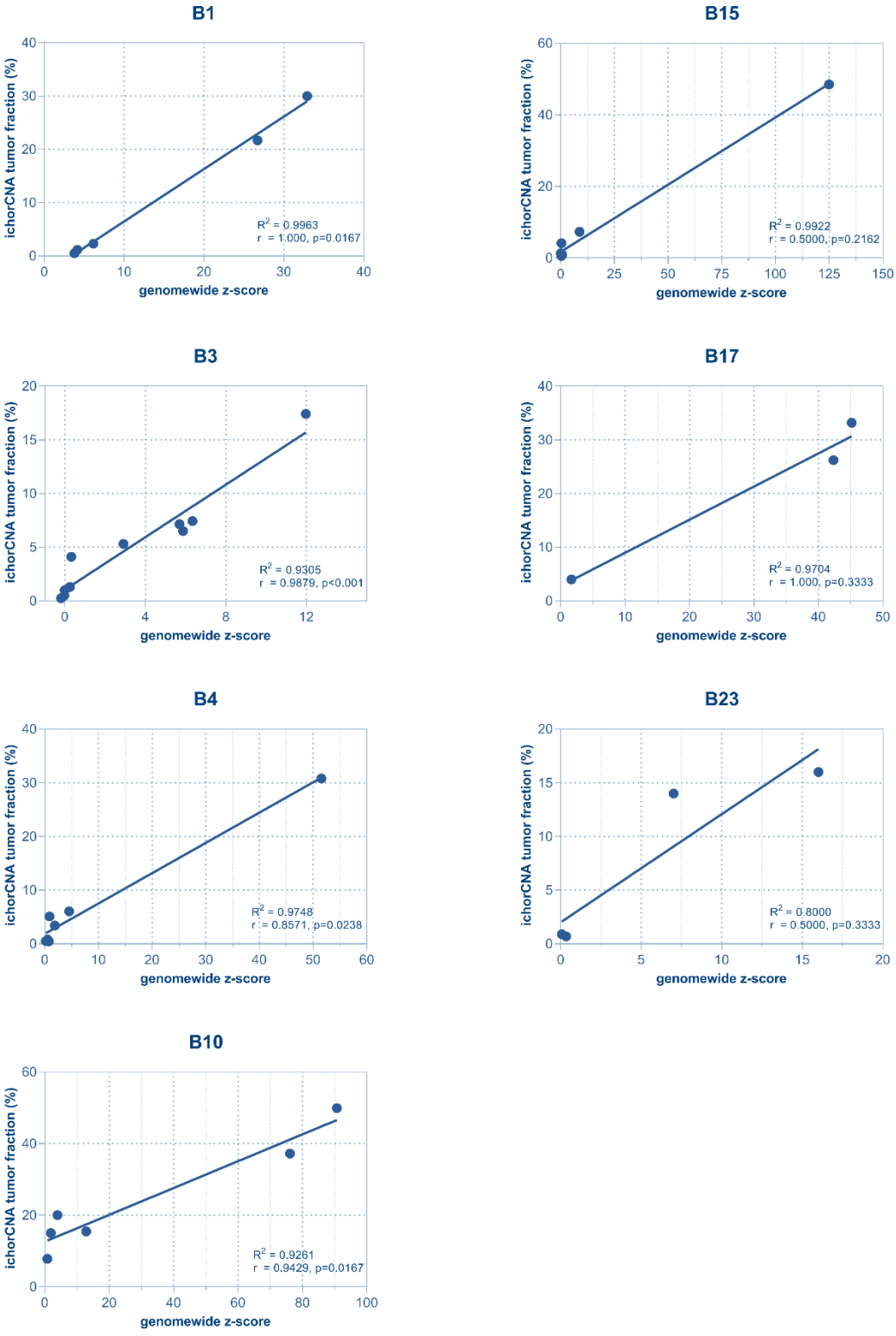

Figure 5. Correlation between mFAST-SeqS z-scores and ichorCNA-based tumor fractions in seven patients (as published in (130))

3.1.3 Prognostic impact on survival

We stratified patients according to their baseline z-scores in order to evaluate whether the level of aneuploidy and/or high tumor fractions in plasma was associated with survival. A z-score cut-off of 3 was found to be most suitable to predict OS and PFS. The OS of 10 patients with a z-score ≥ 3 (16.0 months; 95% CI 6-32 months; log-rank test, $p = 0.014$; Figure 3B) was significantly lower than in 19 patients with a z-score < 3 (median not reached).

Kaplan-Meier's estimates of OS of two years stated: 40% for patients with a z-score ≥3 and 79% for patients with a z-score <3. Also, patients with elevated z-scores showed a significantly shorter PFS compared to patients with z-scores < 3 proved (Figure 6A).

Baseline CTC counts, CEA or CA15-3 were not associated with PFS or OS, respectively (Figure 7). In a multivariate model, z-score was not an independent prognostic factor mostly due to the small sample size.

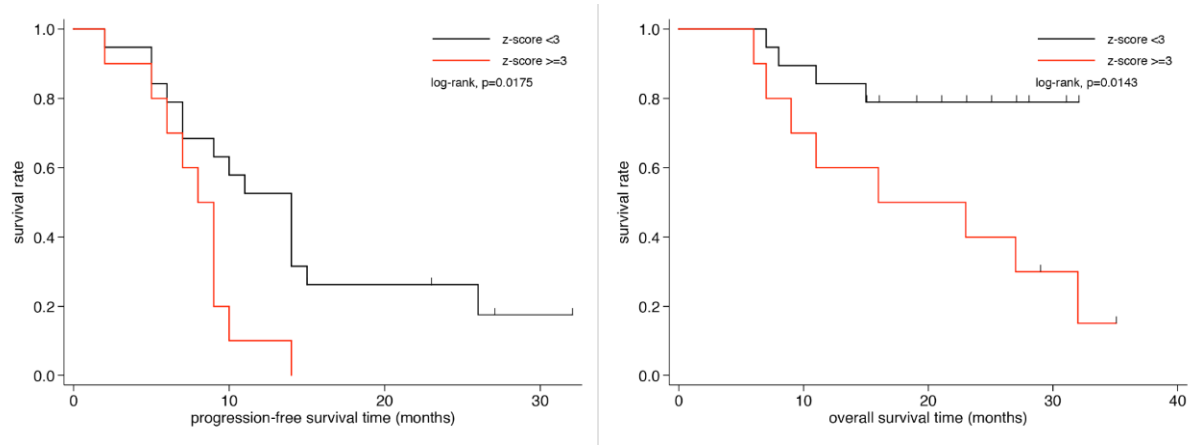

Figure 6. PFS and OS according to z-scores in metastatic breast cancer patients (as published in (130))

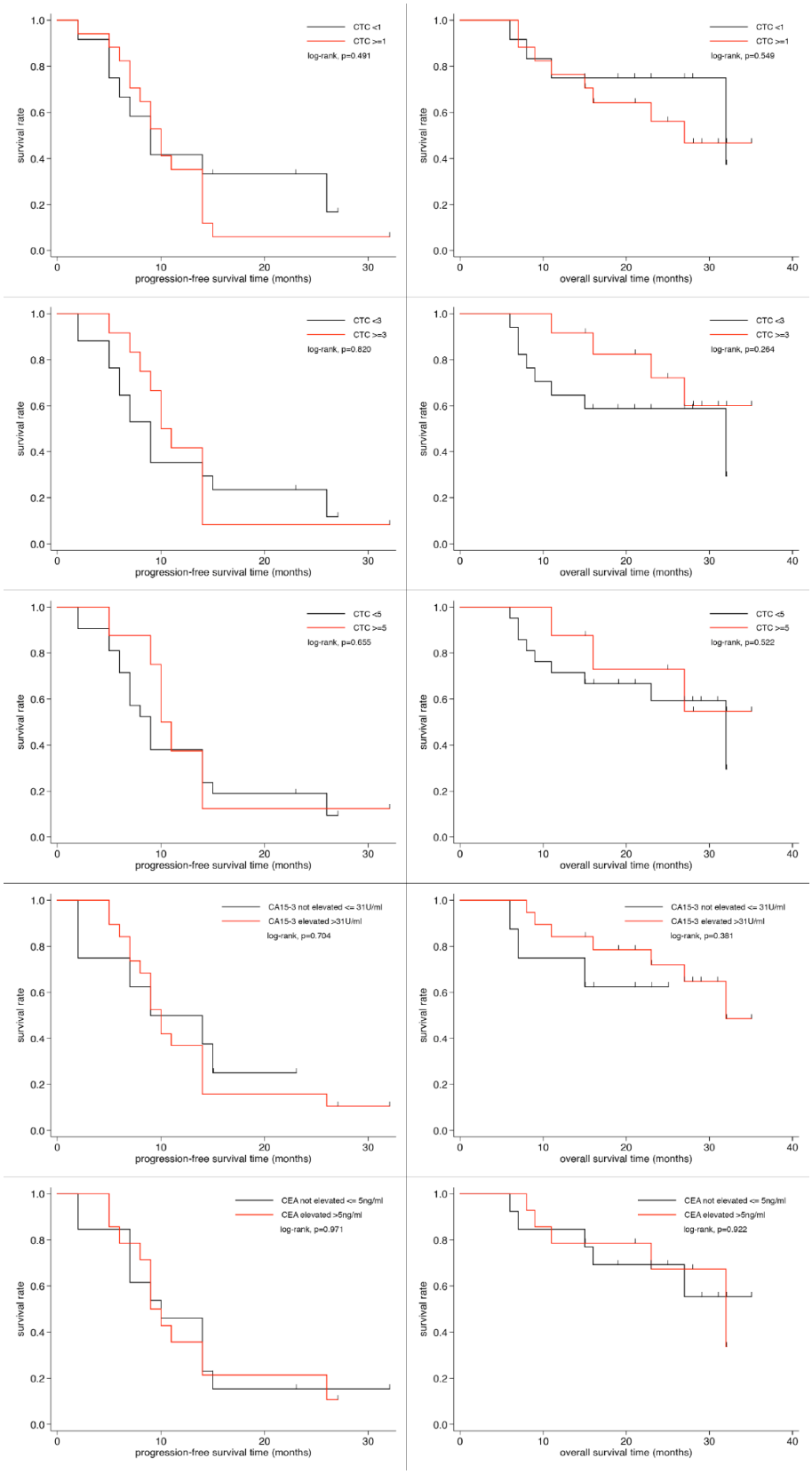

Figure 7. PFS and OS based on CTC status, CEA and CA15-3 levels (as published in (130))

3.1.4 Association of tumor fractions, CTC detection rate, tumor marker and clinicopathological characteristics

In 14 out of 27 (51.9%) and 19 out of 27 (70.4%) patients we found increased levels of CEA (>5ng/ml) and CA15-3 (>31U/ml) at baseline, in 2 patients it was not determined. A z-score of ≥ 3 at baseline was detected in only 10 out of 29 patients (34.5%). At the same time a total of 17/29 patients (58.6%) showed ≥ 1 CTC at baseline.

ctDNA and CTC for comparison were available from 29 patients, for 97 samples. A z-score ≥ 3 was found in 31 out of 97 samples (32.0%). In 49 out of 97 (50.5%) samples we could detect at least one CTC. Both elevated ctDNA and CTCs were shown in 18 out of 97 (18.6%) analyzed samples. Either a z-score ≥ 3 or one or more CTCs were observed in 62 out of 97 (63.9%) samples. Data comparing ctDNA and tumor markers was available for 29 patients and 112 samples: 41 (36.6%) samples had a z-score ≥ 3, 57 (50.9%) samples had elevated levels for CEA and 76 (67.9%) samples showed increased CA15-3 levels. A z-score ≥ 3 and elevated CEA levels was detected in 25 out of 112 (22.3%) samples. Whereas 34 (30.4%) samples had a z-score ≥ 3 and elevated CA15-3 levels.

The genome-wide mFAST-SeqS z-score and the number of CTCs were not significantly associated. ctDNA and tumor markers as well as CTC count and CA15-3 (Table 3) were significantly correlated. When we connected the tumor fraction and the CTC status at baseline with clinicopathological factors, there was only a significant association between CTC positivity and liver metastasis (Table 4, Table 5).

Table 4. Pairwise correlation matrix of z-score, CTC count, CEA and CA15-3 (as published in (130))

All samples (n=127)	z-score	CTC count	CEA	CA15-3
z-score	-	0.02 (n=97)	0.26 (n=112)	0.25 (n=112)
CTC count	0.02 (n=97)	-	0.01 (n=84)	0.30 (n=84)
CEA	0.26 (n=112)	0.01 (n=84)	-	0.41 (n=111)
CA15-3	0.25 (n=112)	0.30 (n=84)	0.41 (n=111)	-

Statistically significant spearman correlation coefficients (r) are highlighted in bold.

Table 5. Associations of baseline z-score and CTC positivity with clinicopathological characteristics (n=29 patients) (as published in (130))

Variable	z-score < 3	z-score >= 3	P value	CTC <5	CTC >=5	P value
Menopausal status			*1.000*			*0.215*
Premenopausal	10	5		9	6	
Postmenopausal	9	5		12	2	
Histology			*0.592*			*0.304*
IDC/NST	17	8		17	8	
others	2	2		4	0	
Tumor grading			*0.714*			*0.697*
Grade 1/2	8	5		10	3	
Grade 3	11	5		11	5	
Tumor size (pT)[#]			*0.252*			*0.121*
pT1	7	3		9	1	
pT2	3	6		5	4	
pT3/4	3	1		4	0	
Lymph nodes (pN)*			*1.000*			*1.000*
pN0	5	5		8	2	
pN1-3	7	5		9	3	
ER status			*0.306*			*0.597*
Negative	2	3		3	2	
Positive	17	7		18	6	
PR status			*1.000*			*1.000*
Negative	6	3		7	2	
Positive	13	7		14	6	
HER2 status			*0.675*			*1.000*
Negative	13	8		15	6	
Positive	6	2		6	2	
Subtype (primary tumor)			*0.065*			*1.000*
HR+/Her2 –	13	5		13	5	
HR-/Her2-	0	3		2	1	
Her2+	6	2		6	2	
Bone metastases			*1.000*			*0.371*
No	6	3		8	1	
Yes	13	7		13	7	
Lung metastases			*0.270*			*0.406*
No	12	4		13	3	
Yes	7	6		8	5	
Liver metastases			*0.244*			*0.001*
No	14	5		18	1	
Yes	5	5		3	7	

[#]pT was not available for 6 patients; *pN status was not available for 7 patients

3.1.5 Serial monitoring of the genome-wide z-score of ctDNA

We finally examined whether quantitative changes in mFAST-SeqS z-scores during treatment may reflect the response to therapy and disease progression. 108 individual plasma samples (mean 3.7, range 1-8) were analyzed. For the following estimates we used a linear mixed model with a random intercept at the patient level: the mean z-scores at baseline were 8.21 (95%CI: 1.91-14.52), 2.81 (95%CI: -1.77-7.39) during treatment, and 17.56 (95%CI: 8.82-26.29) at disease progression (Wald test, p=0.007). Higher z-scores were significantly associated with disease progression compared to treatment z-scores (Wald test, p=0.002). At the same time we did not find any difference between mean baseline z-scores and mean treatment z-score (Wald test, p=0.150). Also, CA15-3 showed similar results. Whereas neither CEA nor CTCs showed any significant difference at these time points (Figure 8).

Changing levels of tumor fraction based on z-scores were detected in 13 patients (46%). On the other hand there were 15 patients (54%) showing z-scores < 3 for all analyzed time points although disease progression was diagnosed.
However, in patients with at least one elevated z-score, there was an association between z-score assessment and radiological response to therapy (Figure 9, Figure 10). Most of the time they had z-scores > 3 when tumor treatment was started resulting in a decrease according to the radiological response. In case of progressive disease, we could note an increase of z-scores or still elevated levels (Figure 9, Figure 10). This was also seen for ichorCNA tumor fractions: dynamics of CA15-3 levels showed a close correlation with a ctDNA fraction and the z-score, while CEA levels did not provide informative results.

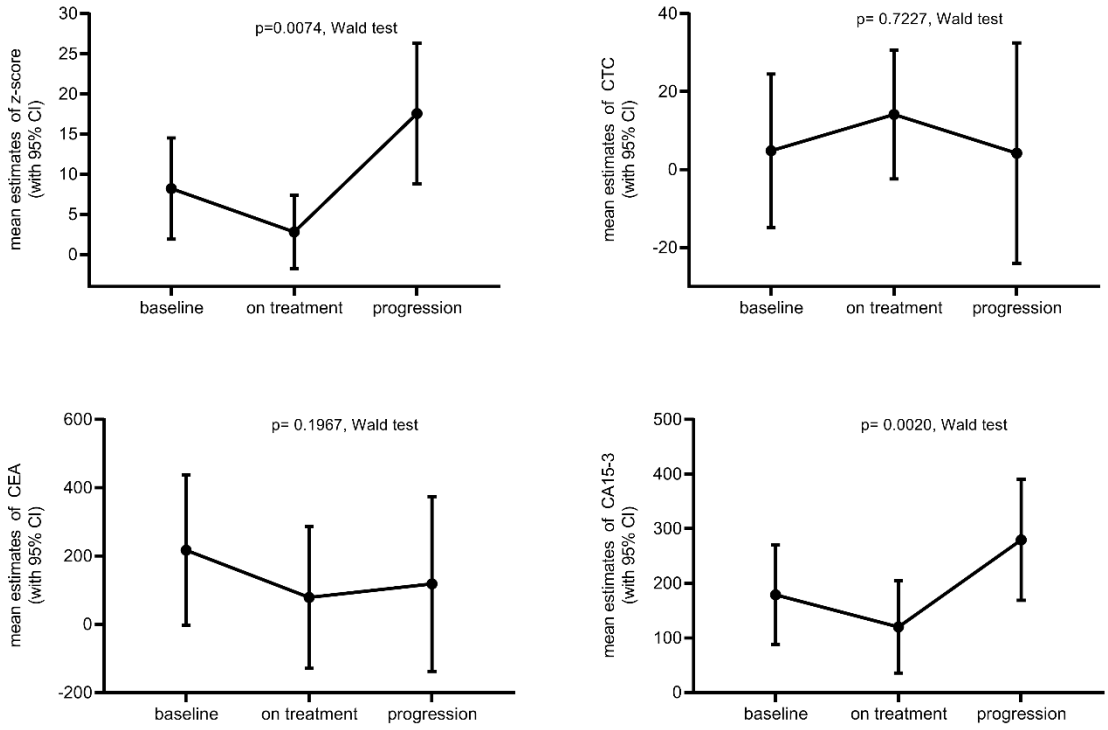

Figure 8. Mean estimates of z-scores, CTC counts, CEA and CA15-3 levels during treatment (as published in (130))

CA15-3 levels and z-scores were significantly increased at disease progression compared to baseline and treatment. There was no significant difference between CTC counts and CEA at the three time points.

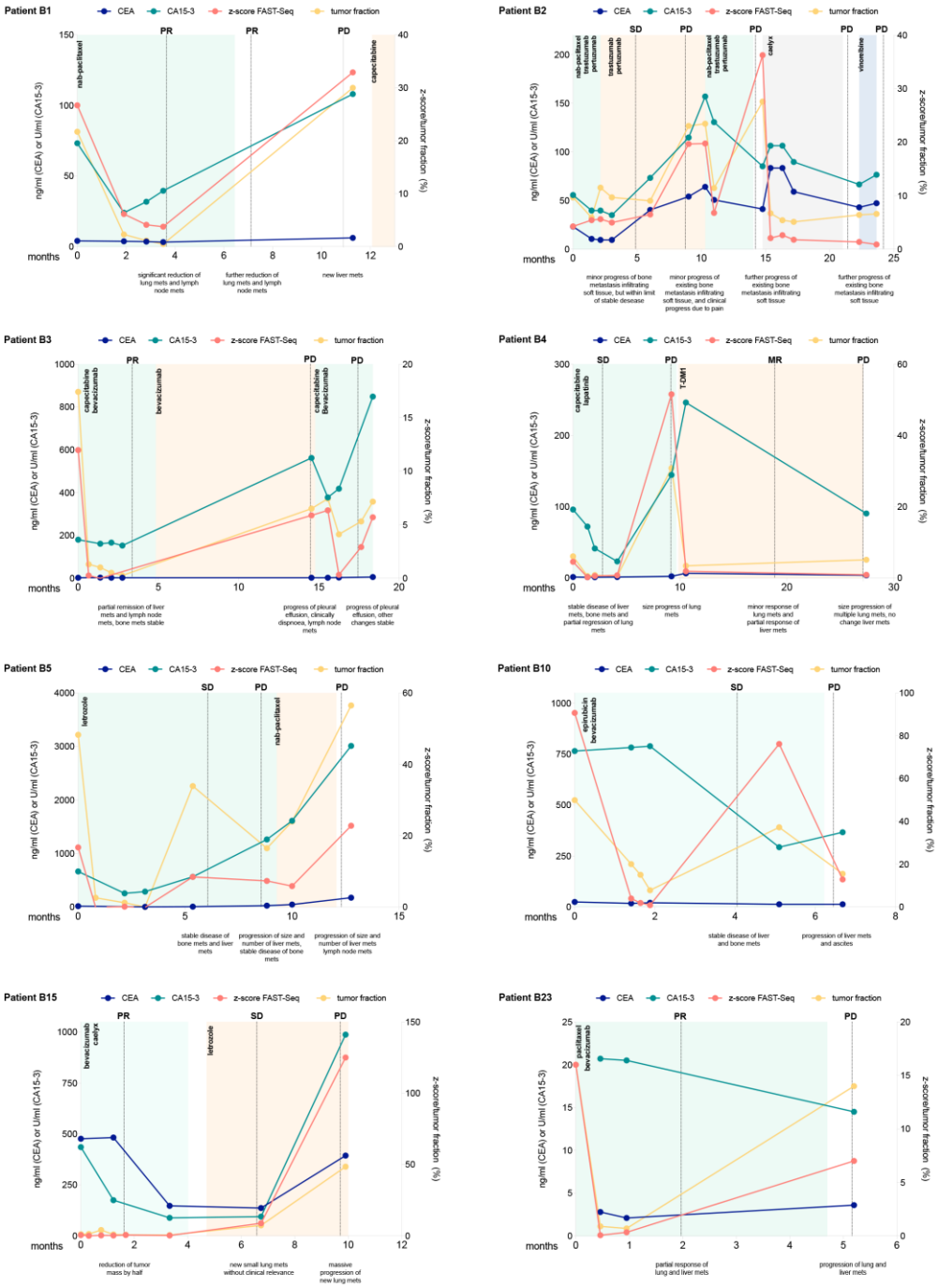

Figure 9. Longitudinal monitoring of z-scores and ichorCNA tumor (as published in (130))

Different treatments are shown in colored shading, response to therapy is shown as vertical dotted lines. SD stable disease, PD progressive disease, PR partial response, MR minor response.

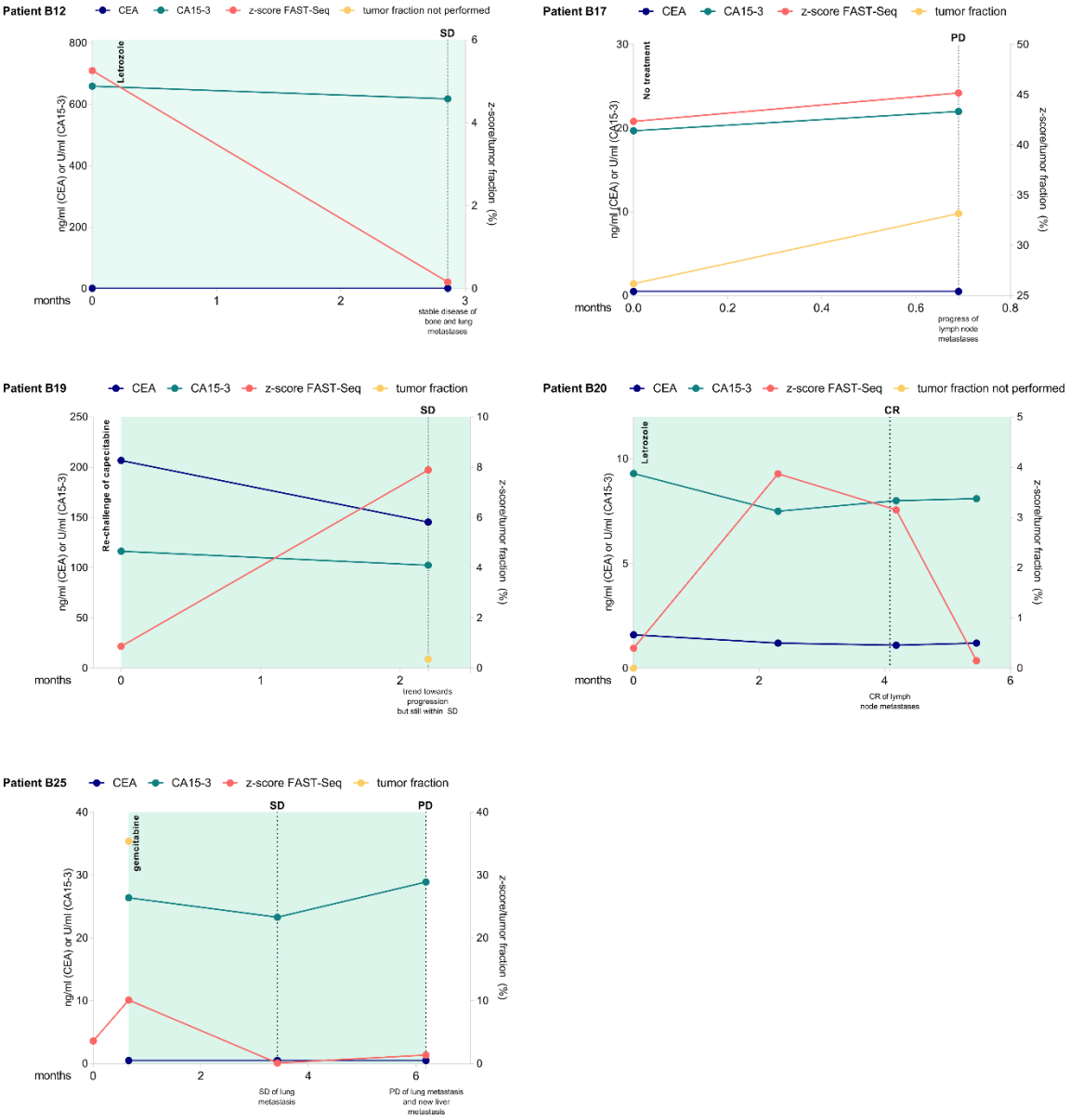

Figure 10. Longitudinal monitoring of z-scores (as published in (130))

SD stable disease, PD progressive disease, CR complete response.

3.2 Project 2

This section is part of a work that has been submitted for publication.

3.2.1 Patient characteristics

Seventy patients were enrolled, and sixty-nine advanced or metastatic HR positive, Her-2 negative breast cancer patients with a median age of 65.4 years [25th-75th percentile: 57.3-76.6] were analyzed in this study. These patients were planned for antihormonal treatment in combination with a CDK 4/6 inhibitor. Table 6 shows the main patients' characteristics. The majority of patients were female (94.2%) and had HR+/HER2- tumors (92.8%). The most frequent metastatic site was bone (65.2%), followed by lymph nodes (34.8%), lung (31.9%), liver (21.7%), and pleura (10.1%). Forty-one patients (59.4%) had multiple metastatic sites, and the majority of patients (79.7%) received first or second-line palliative treatment at study inclusion. Sixty-five tissue samples and 67 plasma samples were available for *PIK3CA* mutation analysis (Figure 11). For the comparison cohort consisting of 63 paired tissue and plasma samples, the median time interval between tissue and plasma sample collection was 6.6 months [25th–75th percentile:0.7-46.6 months].

Table 6. Baseline characteristics of the study population (N=69)

	Total cohort N=69
Age at inclusion (years)	65.4 (57.3-74.6)
Female gender	65 (94.2%)
Histological type	
IDC/NST	43 (61.4%)
ILC	17 (24.3%)
Other or not reported	10 (14.3%)
Molecular subtype	
HR+/HER2-	64 (92.8%)
Triple positive	3 (4.3%)
Triple-negative	2 (2.9%)
Bone metastases	45 (65.2%)
Lung metastases	22 (31.9%)
Liver metastases	15 (21.7%)
Pleura metastases	7 (10.1%)
Lymph node metastases	24 (34.8%)
Number of metastatic sites	
0-1 sites*	28 (40.6%)
≥ 2 sites	41 (59.4%)
Treatment line at inclusion	
≤ 2 lines	55 (79.7%)
>2 lines	14 (20.3%)
PIK3CA mutation detected in plasma (N=67)[a]	34 (50.7%)
PIK3CA mutation detected in tissue (N=65)[b]	32 (49.2%)
Source of tissue	

Metastasis	42 (60.9%)
Primary tumor	27 (39.1%)
Interval between tissue and blood sample collection (months)	6.6 (0.7-41.8)

Data are medians [25th-75th percentile] for continuous data and absolute frequencies (%) for count data. [a]NGS failed in two plasma samples. [b] No sufficient tumor material was available for NGS testing in four cases. *Includes one patient with locally advanced disease.

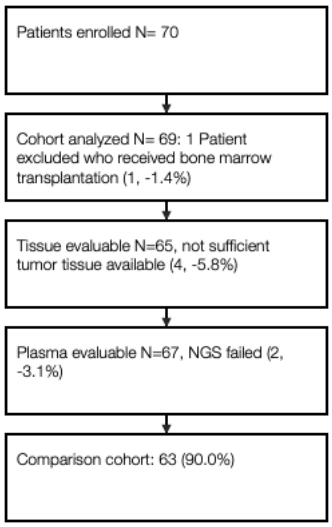

Figure 11. Plasma samples for PIK3CA analysis

3.2.2 *PIK3CA* mutations and z-scores in patients with evaluable plasma samples (N=67)

Of all 67 patients with evaluable plasma samples, 50.7% (34/67) had detectable *PIK3CA* mutations. In detail, 41 *PIK3CA* mutations were detected, and in seven samples, the co-occurrence of two *PIK3CA* mutations was observed. Double or compound *PIK3CA* mutations are described in cis on the same allele; they are supposed to increase PI3K activity and enhance downstream signaling, cell proliferation, and tumor growth (140). The VAF of detected *PIK3CA* mutations in plasma ranged from 0.28 to 49.85%, with a median of 1.17%. The most frequent mutation reported in the *PIK3CA* positive plasma samples was H1047R (58.6%), followed by E542K (26.8%) and E545K (14.6%).

Patients with *PIK3CA* mutated ctDNA were less likely to have lung metastases (*p=0.027*). Other metastatic sites, including bone, liver, and lymph nodes, were not significantly associated with *PIK3CA* mutated ctDNA. Similarly, multiple metastases were also not significantly associated with *PIK3CA* mutations. Finally, there was no difference between the line of treatment and the presence of *PIK3CA* mutations in plasma.

The median z-score resulting from mFAST-SeqS analyses was 2.21 [25th -75th percentile: 1.59-6.34]. Based on a previously established cut-off at ≥ 3, which depending on the amount and amplitude of copy number alterations, correlates to a tumor fraction of 5-10% (130), 26/67

(38.8%) patients had elevated z-scores. We found no statistically significant correlation between z-scores and mutant *PIK3CA* allele frequencies (Spearman r = -0.17, *p=0.174*). Surprisingly, z-scores were higher in samples where no *PIK3CA* mutation was detected (median 3.28, range 0.85-37.46) compared to *PIK3CA* mutated samples (median 1.82, range 0.77-16.59; Wilcoxon rank-sum test *p=0.0120*; Figure 12). More than half of the patients with no detectable *PIK3CA* mutation (18/33, 54.6%) presented z-scores ≥3, indicating a high tumor content. Since ctDNA but no *PIK3CA* mutation could be detected in these samples, they can be considered true negatives for the assessed *PIK3CA* mutations. In contrast, for 15 patients with low (<3) z-scores and, therefore, low tumor fractions in plasma, the presence of *PIK3CA* mutations below the LOD cannot be entirely excluded. In these cases, tissue-based *PIK3CA* analysis might be indicated. Taken together, in 15 out of 67 patients (22%), the *PIK3CA* status was negative and z-score<3 based on ctDNA analyses. For these 15 patients, 14 tissue samples were evaluable for *PIK3CA* testing, and *PIK3CA* mutations were detected only in 3/14 patients.

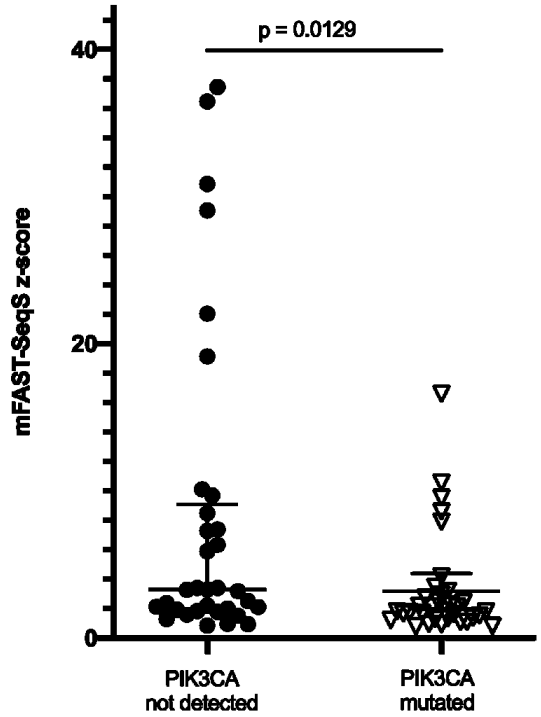

Figure 12. Comparison of genome-wide z-scores in plasma samples by PIK3CA mutation status

Symbols (circles and triangles) represent z-scores for individual patients. Error bars depict the median with interquartile range. The p-value is from a Wilcoxon sign-rank test.

3.2.3 *PIK3CA* mutations in patients with evaluable tissue samples (N=65)

PIK3CA mutations were detected in 49.2% of archival tumor tissue (27 primary, 38 metastatic). VAF ranged from 4.36 to 72.93% (median 28.60%). The most frequent *PIK3CA* mutation detected in tissue was H1047R (43.8%), followed by E545K (31.2%), E542K (18.8%), and H1047L (6.2%). In contrast to plasma, there were no patients with double *PIK3CA* mutations in tissue. The frequency of liver metastases was lower in patients with *PIK3CA* mutations in tissue, but this trend did not reach statistical significance (*p=0.081*). Similarly, multiple metastases were numerically associated with *PIK3CA* mutations, but this association was not significant (*p=0.097*). Bone, lung, lymph node metastases, and treatment lines were not associated with *PIK3CA* mutations in tissue samples.

3.2.4 Concordance of *PIK3CA* mutation status in plasma and tissue

Comparative analyses of plasma and tissue were performed from 63 patients for the 11 *PIK3CA* hot spot mutations covered by both assays (Figure 13). We found a good agreement between tissue and plasma samples, with a Cohen kappa = 0.63 (95% CI, 0.561-0.695) and an overall concordance rate of 76.2% (48/63,Table 7). Overall concordance was similar if only metastatic tissue samples (28/37, 75.7%) or only primary tissue samples (20/26, 76.9%) were considered. In detail, 22/63 patients (34.9%) had the same *PIK3CA* alteration in plasma and tissue, while no *PIK3CA* mutation in neither sample type was found in 26/63 patients (41.3%). Discordant results (15/63, 23.8**%;** Table 8) included seven patients with a *PIK3CA* mutation in plasma only and five patients with a *PIK3CA* mutation in tissue only. In addition, in three patients, a different *PIK3CA* mutation was detected in the plasma sample compared to the tissue sample. The overall comparison showed no statistical difference between the results of tissue and plasma (McNemar's test *p=0.564*). For concordant samples, the *PIK3CA* VAF in ctDNA were generally higher (median 2.49, range 0.37-17.70) than for the discordant samples (median 0.77, range 0.31-1.25; Wilcoxon rank-sum test *p=0.006*), where mutations where only detected in plasma (Figure 13). Similarly, z-scores were numerically but not statistically significantly lower in discordant samples (median 1.75, range 0.77-7.90) compared to concordant samples (median 2.37, range 0.85-37.46; Wilcoxon rank-sum test *p=0.088*). Additionally, only four out of the 15 discordant samples had z-scores ≥3. Finally, the time interval between plasma and tissue collection did not significantly differ and ranged from -9.9 to 139.2 months (median 2.3 months) for discordant samples and from -14.8 to 229.1 months (median 8.7 months) for concordant samples (Wilcoxon rank-sum test *p=0.474*).

Overall, thirty-nine *PIK3CA* mutations were detectable in plasma samples of 32/63 patients (50.8%), compared to 30 *PIKC3A* mutations in tissue samples of 30/63 patients (47.6%). In seven plasma samples, double *PIK3CA* mutations were detected, while no double mutations occurred in tumor tissue samples. H1047R was the most frequent mutation found in both plasma and tissue samples (65.6% in plasma, 46.7% in tissue), followed by E545K (9.5% in plasma, 12.7% in tissue) and E542K (7.9% in plasma, 9.5% in tissue). The H1047L variant was detected in two tissue samples (3.2%) but not in plasma samples.

Focusing only on the question of whether we were able to identify patients qualifying for alpelisib treatment based on the detection of any of the 11 *PIK3CA* mutations included in the SOLAR-1 trial, we detected at least one mutation in 37/63 patients both in tissue and plasma. In 7 patients, such mutations were found only in plasma. Within five patients with tissue *PIK3CA* mutations not detectable in ctDNA, two patients had low tumor fractions (z-score<3). Comparing our results to the liquid biopsy-based results in the SOLAR-1 study, we found that the proportions of discordant plasma samples compared to wild-type tissue samples were significantly higher in our study ($p<0.001$). In contrast, the proportion of discordant plasma samples compared to mutant tissue samples was significantly lower in our study ($p=0.001$, Figure 14). (https://www.accessdata.fda.gov/cdrh_docs/pdf19/P190004B.pdf) These results indicate that our SIMSenSeq assay was more sensitive than the TheraScreen Assay used in the SOLAR-1 study.

Finally, we performed an exploratory analysis assessing the association between *PIK3CA* mutation and progression-free survival in a subset of 47 HR+/HER2+ breast cancer patients receiving CDK inhibitor treatment. In this subset of patients, the presence of a *PIK3CA* mutation in plasma was not significantly associated with PFS (HR 1.25, 95%CI 0.54-2.90, $p=0.604$; Figure 15)

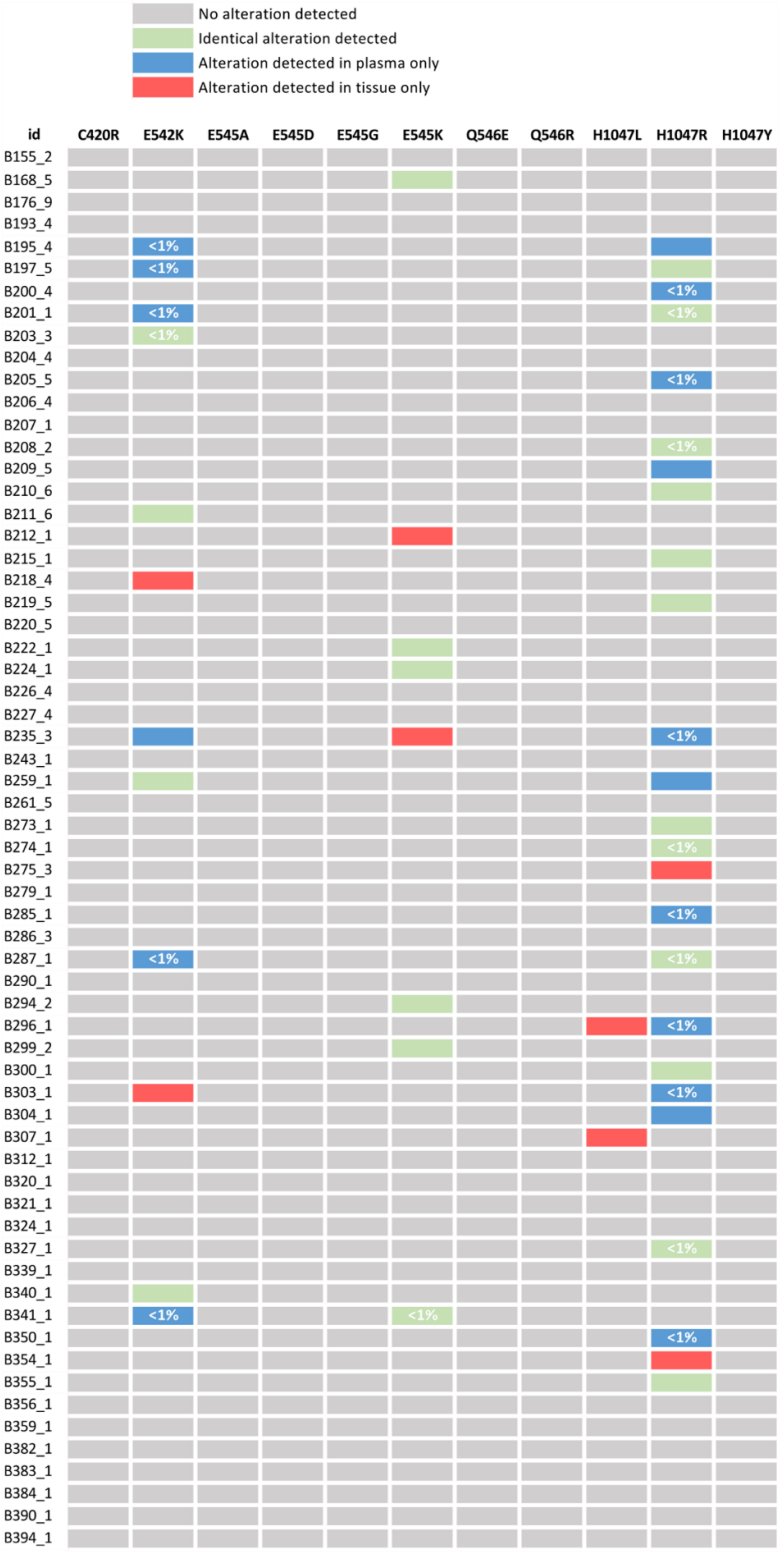

Figure 13. Landscape of PIK3CA alterations in plasma and tissue samples of the comparison cohort (N=63)

Each row represents one patient, and only PIK3CA hot spot mutations covered by both assays were considered for the comparison. <1% denotes plasma samples with allele frequencies below 1%

Table 7. Summary of PIK3CA mutation concordance data comparing plasma with tissue samples (N=63)

	No	%
Total concordance (no alteration or identical alteration)	**48**	**76.2**
No alterations found in plasma and tissue	26	41.3
Identical alterations found in plasma and tissue	22	34.9
Total discordant samples	**15**	**23.8**
Different alterations found in plasma and tissue	3	4.8
Plasma only	7	11.1
Tissue only	5	7.9
Total number of alterations found in tissue	30	-
Total number of alterations found in plasma	39	-
Samples with double mutations in tissue	0	0.0
Samples with double mutations in plasma	7	11.1

Table 8. Discordant PIK3CA mutation results (N=15) between plasma and tissue samples

Patient ID	Mutation(s) in Plasma (AF %)	z-score	Mutation in Tissue (MAF %)	Source of Tissue	Time interval between plasma and tissue collection*
B195	H1047R (1.25), E542K (0.34)	4.18	ND	metastasis	6 days
B200	H1047R (0.98)	1.75	ND	metastasis	4.4 months
B205	H1047R (0.72)	7.90	ND	metastasis	14 days
B209	H1047R (1.17)	1.22	ND	primary	6.6 months
B212	ND	3.19	E545K (30.7)	primary	-9.9 months
B218	ND	3.40	E542K (23.7)	metastasis	16.1 months
B235	E542K (1.34), H1047R (0.77)	1.69	E545K (49.2)	primary	22.6 months
B275	ND	2.51	H1047R (25.5)	primary	2.2 months
B285	H1047R (0.31)	1.81	ND	metastasis	-4.6 months
B296	H1047R (0.58)	0.77	H1047L (30.5)	metastasis	2.3 months
B303	H1047R (0.42)	0.81	E542K (29.5)	metastasis	7 days
B304	H1047R (1.08)	2.20	ND	primary	139.2 months
B307	ND	1.51	H1047L (25.9)	primary	88.5 months
B350	H1047R (0.47)	1.29	ND	metastasis	1.8 months
B354	ND	0.94	H1047R (15.9)	metastasis	119.0 months

ND no mutation detected; *negative numbers mean that plasma samples were analyzed at an earlier date than tissue samples

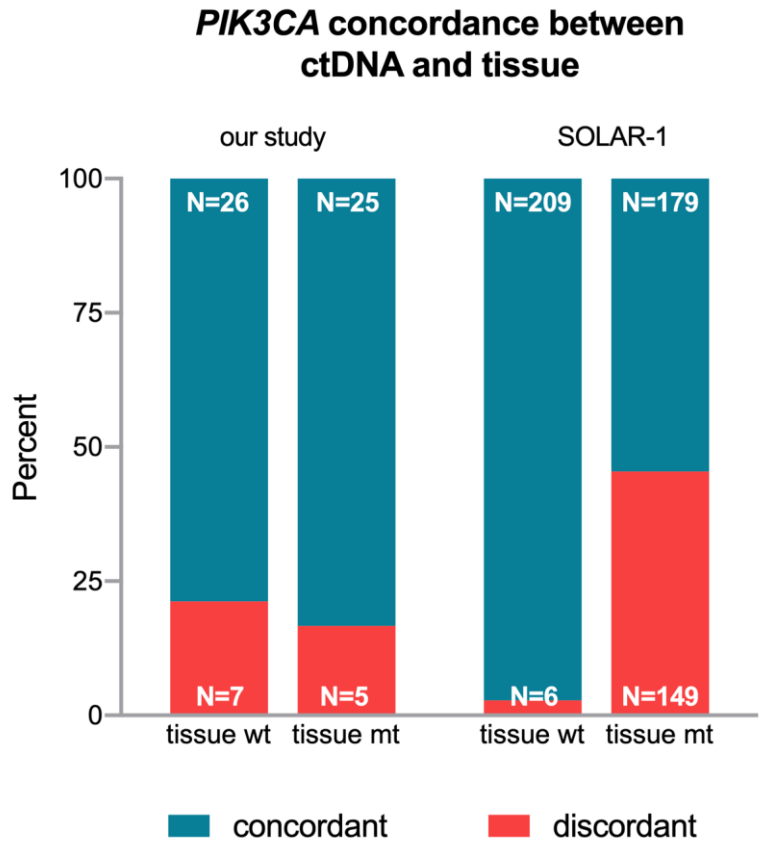

Figure 14. PIK3CA concordance between ctDNA and tissue

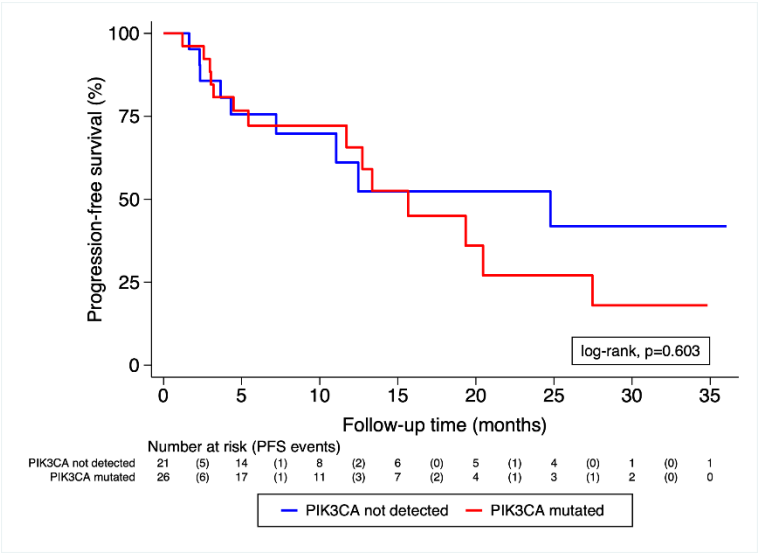

Figure 15. Progression-free survival by PIK3CA mutation status in plasma. Curves were estimated with Kaplan-Meier estimators

4 Discussion

The present thesis demonstrates clinical utility of ctDNA analyses in two different ways. First the value of untargeted mFAST-SeqS and derived z-score for determination of the tumor fraction and its applicability for monitoring of therapeutic response. Second, its role in combination with targeted SimSen-Seq for determination of patients with *PIK3CA* mutations as possible candidates for treatment with alpelisib. With those two approaches ctDNA analyzed proofs helpful in guiding treatment decisions in metastatic hormone receptor positive patients.
Below, these two projects are first discussed separately, and then conclusions for the future studies are summarized.

4.1 Project 1

Tumor fraction in plasma associated with prognosis has already been shown in several tumor entities (141-145). In metastatic setting, a recent metastatic biopsy is not always available for analysis, whereas a liquid biopsy can be easily performed. There is without a doubt the need for an untargeted assessment of the tumor load without a priori knowledge of specific changes of the tumor in the circulation. Taking into account that metastases differ from primary cancers in their driver landscape (146).

In this dissertation the untargeted assessment of tumor fraction using the mFAST-SeqS method provides important information for both prognosis and treatment response in patients with metastatic breast cancer. A z-score ≥ 3 before start of a treatment line was associated with worse OS and PFS while at the same time CTCs, CA15-3 levels or CEA levels did not add prognostic information.
Especially regarding to CTCs, the heterogenous patient population, small number of samples as well as differences in methods of CTC enrichment and detection may be an explanation for these results. Moreover CTC detection was based on CK expression, a possible reason why CTCs in epithelial-mesenchymal transition (EMT) or with stem cell character could have been missed. Notably we believe that this study was underpowered to answer this certain question while there are data showing the prognostic role of CTC detection. There is necessarily the need of a trial enrolling a more homogenous patient population with a larger sample size in the near future. In spite of these limitations, z-score based DNA levels did add significant prognostic information and their informative role should be further investigated and confirmed.

Comparable results confirming the prognostic value for mFAST-SeqS were also seen in patients with prostate cancer (141). This indicates that elevated tumor fractions may be independently prognostic in different tumor types. Adalsteinsson et al presented data on ichorCNA (134), an analytical approach that quantifies tumor fraction in cfDNA from ultra-low-pass whole-genome-sequencing. It is possible to estimate cfDNA samples with tumor content over 10% for whole-exome sequencing by using this approach. A retrospective cohort study on 164 patients with triple-negative breast cancer used ichorDNA to stratify them on the basis of tumor fractions with a threshold of ≥ 10%. Comparable to our presented data used in my thesis high tumor fractions were significantly correlated to worse survival. This again confirms elevated tumor fractions in the plasma of metastatic breast cancer patients being of prognostic significance (142).

In my opinion z-scores represent the longitudinal assessment of changing levels of ctDNA in individual patients very well. Given the fact that there was a strong correlation between quantitative changes of z-scores and tumor fractions within samples from the same patient. This has been confirmed by analyzing mFAST-SeqS as a monitoring tool. In most cases radiologically confirmed progress was associated with elevated z-scores in patients with informative values, while efficacy of therapy as a radiologic response correlated with significantly lower z-scores. However, the change of CTCs or CEA levels in this study was not to be associated with response to tumor therapy. The small sample size as well as the heterogeneity of the patient cohort limited the outcome of this study.

mFAST-SeqS resolution is limited to SCNA calling at chromosome-arm levels and the need of *LINE*1 sequences within the altered region, thereby differing from other WGS approaches. The analytical sensitivity is, of course, one limitation of this method, coming into use in more advanced settings, usually associated with elevated ctDNA levels. These advanced settings represent a field of interest and an area where several trials are being performed. That is why this approach has great potential to become part of a diagnostic tool for studies in these settings. The increase of the sequencing depth or bioinformatic approaches result in an improvement of sensitivity. Douville et al published an improved *LINE1*-based method called Within-Sample Aneuploidy Detection (WALDO). This algorithm incorporates machine learning in order to detect somatic mutations, allelic imbalances or microsatellite instability and is suitable in cases when smaller amounts of DNA are available (147).

Nevertheless, there are several advantages of mFAST-SeqS compared to other ctDNA analysis methods. First of all it is a fast method being performed within 24 hours given the fact that it is a two-step PCR. Second it is an affordable method: given the minimum number of

reads of 100.000, analysis can be done on a benchtop sequencer like the MiSeq or MiniSeq. One MiSeq run includes a maximal pooling of six samples as a result of about 3 – 4 million reads in order to determine a reliable copy number profiling. An additional advantage is its application to a wide range of tumors because mFAST-SeqS is based on genome-wide SCNAs rather than specific mutations given the fact that almost all solid tumors are genetically instable. When performing WGS libraries there is the need of 5-10ng template DNA while 500pg -1ng as a minimal amount of plasma DNA is enough for mFAST-SeqS. In summary, mFAST-SeqS is a useful and fast tool for untargeted assessment of tumor fraction in metastatic breast cancer patients in order to estimate both prognosis und treatment response and should be further validated in larger well-defined cohorts.

4.2 Project 2

This analysis with patient-paired plasma and tissue samples shows that a liquid biopsy-based approach holds promise to identify patients with the most common activating *PIK3CA* mutations. Using the high-resolution NGS-based SiMSen-Seq approach, *PIK3CA* mutations were detected non-invasively in over 50% of our patients with a high concordance to tissue data. A combination with an untargeted, mutation-independent approach for detecting ctDNA fractions might confirm a negative *PIK3CA* result, enhancing the performance of the SiMSen-Seq test. This approach allowed the optimization of the selection of candidate patients for *PIK3CA* targeted treatment.

The concept of ctDNA based detection of *PIK3CA* mutations as predictive biomarkers for the PI3K inhibitors was already evaluated in the phase III trials BELLE-2 and BELLE-3 with the Pan-PI3K inhibitor buparlisib (48, 148) and in the SANDPIPER trial with the alpha-specific PI3K inhibitor taselisib (149). Due to the toxicity profile and the magnitude of benefit, neither buparlisib nor taselisib have been clinically developed further in HR+/HER2- breast cancer. Nevertheless, *PIK3CA* mutation testing based on liquid biopsy has shown promising results as a predictive biomarker for PI3K inhibitors (150). The data was confirmed more recently in the SOLAR-1 trial (51). *PIK3CA* mutations in ctDNA did not predict the clinical benefit of everolimus in the BOLERO-2 study. Among 550 patients included in the ctDNA analyses, median PFS was comparable in *PIK3CA* wild type and mutant patients receiving everolimus (50).

The FDA approval of alpelisib includes the companion diagnostic test therascreen® *PIK3CA* RGQ PCR Kit (151), as well as for liquid biopsy testing. Details on the detection of *PIK3CA* mutations in ctDNA in the SOLAR-1 trial have not yet been published. Conference papers refer to the sensitivity of the liquid biopsy-based testing to detect *PIK3CA* mutant patients (152). Out

of 328 patients being identified as positive in the tissue *PIK3CA* mutations could be confirmed in 54.9% of patients in ctDNA via the qPCR assay. The data indicates the sensitivity of the test performed in patients included in the SOLAR-1 study was substantially lower than the sensitivity of the NGS-based SiMSen-Seq assay used in our study.

By adding the mFAST-SeqS z-score as a surrogate marker for tumor fraction in plasma to the results of SiMSen-Seq, we were able to narrow down the need for tissue testing to only 15 (22%) patients. We identified a *PIK3CA* mutation in the tissue in only three out of these patients with evaluable tissue samples. This finding may be of great importance for ctDNA testing in general since the combination of mutation-specific analyses with an untargeted, fast, and cost-effective assessment of tumor fractions may help data interpretation. In addition to the relevance of its one-time measurement, longitudinal assessment of tumor fractions using mFAST-SeqS sequencing harbors important prognostic information (153).

PIK3CA mutations occur on average in ~40% of HR+ patients with a slightly higher proportion in Luminal A patients (46). In a recent analysis of metastatic breast cancer tissue samples from the SAPHIR study, the positivity of *PIK3CA* mutated samples was lower in the HR+ Her- 2 negative patients, with 28%.

Preliminary data from the AURORA demonstrated a similar overall range of *PIK3CA* mutations in metastatic breast cancer without providing information on the distribution with intrinsic subtypes (53). The activating *PIK3CA* mutations were associated with diminished sensitivity to chemotherapy and worse OS (49). Tzanikou et al. have shown that the frequency of detection of *PIK3CA* mutations in liquid biopsy is higher in metastatic patients than in early stages, possibly either due to a higher proportion of mutated patients but also to higher tumor load in peripheral blood (154). It is reasonable to expect an increase in *PIK3CA* mutations in progressive or recurrent disease (155). We did not observe this increase since the most recent tissue available was used for the NGS, and discordant results were observed independently. Another study demonstrated specifically that the proportion of multiple *PIK3CA* mutated tumors increases with metastatic disease further increasing the importance of continuous testing at the later stage (140). Our results demonstrate that co-occurrence of mutations (e.g., double mutations) were found only in ctDNA substantiating the assumption that DNA may be more representative of the heterogeneity of the disease. However, with our approach, we can neither technically nor biologically confirm that these mutations occurred on the same allele. The VAF of the second mutation was mostly low. Peripheral blood for ctDNA was also partly collected at a later advanced and/ or metastatic stage. A significant proportion of the analyzed tissues (60.9%) was from the most recently biopsied single metastatic lesion. Since compound

mutations were shown to be associated with improved benefit from *PIK3CA* inhibitors, this fact may also be in favor of the definition of *PIK3CA* mutation status based on the ctDNA analyses (140).

The detection of *PIK3CA* mutations in plasma implies the presence of tumor-specific mutations, since germline *PIK3CA* mutations lead to early lethality and are not expected in humans (156). Analytical sensitivity of the assays may allow the detection of very low amounts of mutated DNA with a detection limit of 0.25% VAF in our study. The clinical relevance of detecting very low VAF is not well understood. There are several possibilities for low VAF, including a low tumor DNA fraction and a low proportion of *PIK3CA* mutated cells in the overall tumor mass. With respect to clonality, data suggest that most *PIK3CA* mutations are clonal or truncal mutations (157), leaving the possibility that low tumor ctDNA burden is the major cause of low-level detection. In our study, we observed that discordant samples with low-level VAF were mostly retrieved from patients with low ctDNA burden as measured by z-scores. The correlation between *PIK3CA* VAF levels and clinical benefits from alpelisib, as well as the best time point to start the treatment, is currently unknown, and remains a topic of future studies.

This study has several limitations, including the small sample size, a higher percentage of *PIK3CA* mutated cancers, and the focus on *PIK3CA* mutations only. A broader approach providing information on various important genes would be beneficial, but with a potential of decreased sensitivity for *PIK3CA* mutation detection compared to our present analyses. Future studies of our group will also include a comparison of SiMSen-Seq based detection of *PIK3CA* mutations with NGS technologies analyzing a larger number of genes important for the treatment of metastatic breast cancer, as was recently performed in the plasmaMATCH study (116). Groundbreaking clinical progress was demonstrated for selected metastatic breast cancer patients, we believe that this study paved the way for future large clinical trials. On the other hand, we are in need of establishing precise and low-cost technologies to select patients for currently available PI3K treatments, and our SiMSen-Seq based assay performed well in the current study.

In conclusion of this part of the study, SiMSen-Seq-based detection of *PIK3CA* hotspot mutations from plasma has shown promising results. In combination with an untargeted, mutation-independent approach for detecting ctDNA fractions, I believe that for samples with z- score>3 and no *PIK3CA* hotspot mutations, no additional tissue analyses are needed. Adding ctDNA fractions further increased the validity of negative plasma results. SiMSen-Seq alone and this combinatory approach for plasma analyses substantially improved the robustness of liquid biopsy-based *PIK3CA* mutations testing, particularly compared to the

FDA-approved companion diagnostic test therascreen® *PIK3CA* used in the SOLAR-1 study. This approach should be validated in a larger cohort of patients and compared with larger panel NGS ctDNA sequencing methods to establish the most promising approach for selecting individual treatments for our patients.

4.3 Conclusion

These two independent studies have shown potential clinical applications of liquid-biopsy-based analyses of metastatic breast cancer patients.

In the first study only untargeted assessment of tumor fraction was sufficient to determine prognosis and evaluate treatment response. This data was already tested further in another study performed by our group where we have shown that with implementation of the joint model we can dynamically predict PFS of breast cancer patients in the early metastatic setting (first or second line treatment). It is expected that such analyses together with targeted NGS will facilitate precise treatment of hormone receptor positive metastatic breast cancer patients and support not only clinical trials which are ongoing but also treatment of real-world patients. There is a great potential to use the described approach also in other intrinsic subtypes of breast cancer, and there is an ongoing effort to implement this knowledge in clinical studies. With further work of our group we aim to increase the knowledge to this very promising area of research.

5 Bibliography

1. Ferlay J, Steliarova-Foucher E, Lortet-Tieulent J, Rosso S, Coebergh JW, Comber H, et al. Cancer incidence and mortality patterns in Europe: estimates for 40 countries in 2012. Eur J Cancer. 2013;49(6):1374-403.
2. Waks AG, Winer EP. Breast Cancer Treatment. Jama. 2019;321(3):316.
3. Moinfar F. Essentials of diagnostic breast pathology: a practical approach: Springer Science & Business Media; 2007.
4. Lakhani SR, Ellis IO, Schnitt S, Tan PH, van de Vijver M. WHO Classification of Tumours of the Breast. 2012.
5. Hammond ME, Hayes DF, Dowsett M, Allred DC, Hagerty KL, Badve S, et al. American Society of Clinical Oncology/College of American Pathologists guideline recommendations for immunohistochemical testing of estrogen and progesterone receptors in breast cancer (unabridged version). Arch Pathol Lab Med. 2010;134(7):e48-72.
6. Slamon DJ, Godolphin W, Jones LA, Holt JA, Wong SG, Keith DE, et al. Studies of the HER-2/neu proto-oncogene in human breast and ovarian cancer. Science. 1989;244(4905):707-12.
7. Slamon DJ, Clark GM, Wong SG, Levin WJ, Ullrich A, McGuire WL. Human breast cancer: correlation of relapse and survival with amplification of the HER-2/neu oncogene. science. 1987;235(4785):177-82.
8. Slamon DJ, Leyland-Jones B, Shak S, Fuchs H, Paton V, Bajamonde A, et al. Use of chemotherapy plus a monoclonal antibody against HER2 for metastatic breast cancer that overexpresses HER2. N Engl J Med. 2001;344(11):783-92.
9. Piccart-Gebhart MJ, Procter M, Leyland-Jones B, Goldhirsch A, Untch M, Smith I, et al. Trastuzumab after adjuvant chemotherapy in HER2-positive breast cancer. N Engl J Med. 2005;353(16):1659-72.
10. Foulkes WD, Smith IE, Reis-Filho JS. Triple-negative breast cancer. N Engl J Med. 2010;363(20):1938-48.
11. Cossetti RJ, Tyldesley SK, Speers CH, Zheng Y, Gelmon KA. Comparison of breast cancer recurrence and outcome patterns between patients treated from 1986 to 1992 and from 2004 to 2008. J Clin Oncol. 2015;33(1):65-73.
12. Perou CM, Sørlie T, Eisen MB, van de Rijn M, Jeffrey SS, Rees CA, et al. Molecular portraits of human breast tumours. Nature. 2000;406(6797):747-52.
13. Sotiriou C, Neo SY, McShane LM, Korn EL, Long PM, Jazaeri A, et al. Breast cancer classification and prognosis based on gene expression profiles from a population-based study. Proc Natl Acad Sci U S A. 2003;100(18):10393-8.

14. Sorlie T, Tibshirani R, Parker J, Hastie T, Marron JS, Nobel A, et al. Repeated observation of breast tumor subtypes in independent gene expression data sets. Proc Natl Acad Sci U S A. 2003;100(14):8418-23.
15. Hu Z, Fan C, Oh DS, Marron JS, He X, Qaqish BF, et al. The molecular portraits of breast tumors are conserved across microarray platforms. BMC Genomics. 2006;7:96.
16. Loi S, Haibe-Kains B, Desmedt C, Lallemand F, Tutt AM, Gillet C, et al. Definition of clinically distinct molecular subtypes in estrogen receptor-positive breast carcinomas through genomic grade. J Clin Oncol. 2007;25(10):1239-46.
17. Voduc KD, Cheang MC, Tyldesley S, Gelmon K, Nielsen TO, Kennecke H. Breast cancer subtypes and the risk of local and regional relapse. J Clin Oncol. 2010;28(10):1684-91.
18. Chavez-MacGregor M, Mittendorf EA, Clarke CA, Lichtensztajn DY, Hunt KK, Giordano SH. Incorporating Tumor Characteristics to the American Joint Committee on Cancer Breast Cancer Staging System. The Oncologist. 2017;22(11):1292-300.
19. Swain SM, Kim SB, Cortes J, Ro J, Semiglazov V, Campone M, et al. Pertuzumab, trastuzumab, and docetaxel for HER2-positive metastatic breast cancer (CLEOPATRA study): overall survival results from a randomised, double-blind, placebo-controlled, phase 3 study. Lancet Oncol. 2013;14(6):461-71.
20. Baselga J, Cortes J, Kim SB, Im SA, Hegg R, Im YH, et al. Pertuzumab plus trastuzumab plus docetaxel for metastatic breast cancer. N Engl J Med. 2012;366(2):109-19.
21. Im SA, Lu YS, Bardia A, Harbeck N, Colleoni M, Franke F, et al. Overall Survival with Ribociclib plus Endocrine Therapy in Breast Cancer. N Engl J Med. 2019;381(4):307-16.
22. Senkus E, Kyriakides S, Ohno S, Penault-Llorca F, Poortmans P, Rutgers E, et al. Primary breast cancer: ESMO Clinical Practice Guidelines for diagnosis, treatment and follow-up. Ann Oncol. 2015;26 Suppl 5:v8-30.
23. Cortazar P, Zhang L, Untch M, Mehta K, Costantino JP, Wolmark N, et al. Pathological complete response and long-term clinical benefit in breast cancer: the CTNeoBC pooled analysis. Lancet. 2014;384(9938):164-72.
24. Smith IE, Dowsett M. Aromatase inhibitors in breast cancer. N Engl J Med. 2003;348(24):2431-42.
25. Peto R, Davies C, Godwin J, Gray R, Pan HC, Clarke M, et al. Comparisons between different polychemotherapy regimens for early breast cancer: meta-analyses of long-term outcome among 100,000 women in 123 randomised trials. Lancet. 2012;379(9814):432-44.
26. Piccart-Gebhart MJ, Procter M, Leyland-Jones B, Goldhirsch A, Untch M, Smith I, et al. Trastuzumab after adjuvant chemotherapy in HER2-positive breast cancer. N Engl J Med. 2005;353(16):1659-72.

27. von Minckwitz G, Procter M, de Azambuja E, Zardavas D, Benyunes M, Viale G, et al. Adjuvant Pertuzumab and Trastuzumab in Early HER2-Positive Breast Cancer. N Engl J Med. 2017;377(2):122-31.
28. Martin M, Holmes FA, Ejlertsen B, Delaloge S, Moy B, Iwata H, et al. Neratinib after trastuzumab-based adjuvant therapy in HER2-positive breast cancer (ExteNET): 5-year analysis of a randomised, double-blind, placebo-controlled, phase 3 trial. Lancet Oncol. 2017;18(12):1688-700.
29. von Minckwitz G, Huang CS, Mano MS, Loibl S, Mamounas EP, Untch M, et al. Trastuzumab Emtansine for Residual Invasive HER2-Positive Breast Cancer. N Engl J Med. 2019;380(7):617-28.
30. Liedtke C, Mazouni C, Hess KR, André F, Tordai A, Mejia JA, et al. Response to neoadjuvant therapy and long-term survival in patients with triple-negative breast cancer. J Clin Oncol. 2008;26(8):1275-81.
31. Geels P, Eisenhauer E, Bezjak A, Zee B, Day A. Palliative effect of chemotherapy: objective tumor response is associated with symptom improvement in patients with metastatic breast cancer. J Clin Oncol. 2000;18(12):2395-405.
32. Osoba D. Health-related quality of life as a treatment endpoint in metastatic breast cancer. Can J Oncol. 1995;5 Suppl 1:47-53.
33. Lange CA, Yee D. Killing the second messenger: targeting loss of cell cycle control in endocrine-resistant breast cancer. Endocr Relat Cancer. 2011;18(4):C19-24.
34. Finn RS, Crown JP, Lang I, Boer K, Bondarenko IM, Kulyk SO, et al. The cyclin-dependent kinase 4/6 inhibitor palbociclib in combination with letrozole versus letrozole alone as first-line treatment of oestrogen receptor-positive, HER2-negative, advanced breast cancer (PALOMA-1/TRIO-18): a randomised phase 2 study. The lancet oncology. 2015;16(1):25-35.
35. Rugo H, Finn R, Diéras V, Ettl J, Lipatov O, Joy A, et al. Palbociclib plus letrozole as first-line therapy in estrogen receptor-positive/human epidermal growth factor receptor 2-negative advanced breast cancer with extended follow-up. Breast cancer research and treatment. 2019;174(3):719-29.
36. Turner NC, Ro J, André F, Loi S, Verma S, Iwata H, et al. Palbociclib in hormone-receptor–positive advanced breast cancer. New England Journal of Medicine. 2015;373(3):209-19.
37. Hortobagyi GN, Stemmer SM, Burris HA, Yap Y-S, Sonke GS, Paluch-Shimon S, et al. Ribociclib as first-line therapy for HR-positive, advanced breast cancer. New England Journal of Medicine. 2016;375(18):1738-48.
38. Hortobagyi GN, Stemmer SM, Burris HA, Yap Y-S, Sonke GS, Paluch-Shimon S, et al. Updated results from MONALEESA-2, a phase III trial of first-line ribociclib plus letrozole

versus placebo plus letrozole in hormone receptor-positive, HER2-negative advanced breast cancer. Annals of Oncology. 2018;29(7):1541-7.
39. Verma S, Bartlett CH, Schnell P, DeMichele AM, Loi S, Ro J, et al. Palbociclib in combination with fulvestrant in women with hormone receptor-positive/HER2-negative advanced metastatic breast cancer: detailed safety analysis from a multicenter, randomized, placebo-controlled, phase III study (PALOMA-3). The oncologist. 2016;21(10):1165.
40. Slamon DJ, Neven P, Chia S, Fasching PA, De Laurentiis M, Im S-A, et al. Phase III randomized study of ribociclib and fulvestrant in hormone receptor-positive, human epidermal growth factor receptor 2-negative advanced breast cancer: MONALEESA-3. J Clin Oncol. 2018;36(24):2465-72.
41. Slamon DJ, Neven P, Chia S, Fasching PA, De Laurentiis M, Im S-A, et al. Overall survival with ribociclib plus fulvestrant in advanced breast cancer. New England Journal of Medicine. 2020;382(6):514-24.
42. Sledge GW, Toi M, Neven P, Sohn J, Inoue K, Pivot X, et al. The effect of abemaciclib plus fulvestrant on overall survival in hormone receptor–positive, ERBB2-negative breast cancer that progressed on endocrine therapy—MONARCH 2: a randomized clinical trial. JAMA oncology. 2020;6(1):116-24.
43. Ribnikar D, Volovat SR, Cardoso F. Targeting CDK4/6 pathways and beyond in breast cancer. Breast. 2019;43:8-17.
44. Karakas B, Bachman KE, Park BH. Mutation of the PIK3CA oncogene in human cancers. Br J Cancer. 2006;94(4):455-9.
45. Fruman DA, Chiu H, Hopkins BD, Bagrodia S, Cantley LC, Abraham RT. The PI3K Pathway in Human Disease. Cell. 2017;170(4):605-35.
46. Koboldt DC, Fulton RS, McLellan MD, Schmidt H, Kalicki-Veizer J, McMichael JF, et al. Comprehensive molecular portraits of human breast tumours. Nature. 2012;490(7418):61-70.
47. Saal LH, Holm K, Maurer M, Memeo L, Su T, Wang X, et al. PIK3CA mutations correlate with hormone receptors, node metastasis, and ERBB2, and are mutually exclusive with PTEN loss in human breast carcinoma. Cancer Res. 2005;65(7):2554-9.
48. Di Leo A, Johnston S, Lee KS, Ciruelos E, Lonning PE, Janni W, et al. Buparlisib plus fulvestrant in postmenopausal women with hormone-receptor-positive, HER2-negative, advanced breast cancer progressing on or after mTOR inhibition (BELLE-3): a randomised, double-blind, placebo-controlled, phase 3 trial. Lancet Oncol. 2018;19(1):87-100.
49. Mosele F, Stefanovska B, Lusque A, Tran Dien A, Garberis I, Droin N, et al. Outcome and molecular landscape of patients with PIK3CA-mutated metastatic breast cancer. Ann Oncol. 2020;31(3):377-86.

50. Moynahan ME, Chen D, He W, Sung P, Samoila A, You D, et al. Correlation between PIK3CA mutations in cell-free DNA and everolimus efficacy in HR(+), HER2(-) advanced breast cancer: results from BOLERO-2. Br J Cancer. 2017;116(6):726-30.
51. Andre F, Ciruelos E, Rubovszky G, Campone M, Loibl S, Rugo HS, et al. Alpelisib for PIK3CA-Mutated, Hormone Receptor-Positive Advanced Breast Cancer. N Engl J Med. 2019;380(20):1929-40.
52. Rugo HS, Lerebours F, Ciruelos E, Drullinsky P, Borrego MR, Neven P, et al. Alpelisib (ALP) + fulvestrant (FUL) in patients (pts) with PIK3CA-mutated (mut) hormone receptor-positive (HR+), human epidermal growth factor receptor 2-negative (HER2–) advanced breast cancer (ABC) previously treated with cyclin-dependent kinase 4/6 inhibitor (CDKi) + aromatase inhibitor (AI): BYLieve study results. Journal of Clinical Oncology. 2020;38(15_suppl):1006-.
53. Aftimos PG, Antunes De Melo e Oliveira AM, Hilbers F, Venet D, Vingiani A, Nili Gal Yam E, et al. First report of AURORA, the breast international group (BIG) molecular screening initiative for metastatic breast cancer (MBC) patients (pts). Annals of Oncology. 2019;30:iii48.
54. Diéras V, Miles D, Verma S, Pegram M, Welslau M, Baselga J, et al. Trastuzumab emtansine versus capecitabine plus lapatinib in patients with previously treated HER2-positive advanced breast cancer (EMILIA): a descriptive analysis of final overall survival results from a randomised, open-label, phase 3 trial. Lancet Oncol. 2017;18(6):732-42.
55. Verma S, Miles D, Gianni L, Krop IE, Welslau M, Baselga J, et al. Trastuzumab emtansine for HER2-positive advanced breast cancer. N Engl J Med. 2012;367(19):1783-91.
56. Schmid P, Adams S, Rugo HS, Schneeweiss A, Barrios CH, Iwata H, et al. Atezolizumab and Nab-Paclitaxel in Advanced Triple-Negative Breast Cancer. N Engl J Med. 2018;379(22):2108-21.
57. Antoniou A, Pharoah PD, Narod S, Risch HA, Eyfjord JE, Hopper JL, et al. Average risks of breast and ovarian cancer associated with BRCA1 or BRCA2 mutations detected in case Series unselected for family history: a combined analysis of 22 studies. Am J Hum Genet. 2003;72(5):1117-30.
58. Malone KE, Daling JR, Doody DR, Hsu L, Bernstein L, Coates RJ, et al. Prevalence and predictors of BRCA1 and BRCA2 mutations in a population-based study of breast cancer in white and black American women ages 35 to 64 years. Cancer Res. 2006;66(16):8297-308.
59. Robson M, Im SA, Senkus E, Xu B, Domchek SM, Masuda N, et al. Olaparib for Metastatic Breast Cancer in Patients with a Germline BRCA Mutation. N Engl J Med. 2017;377(6):523-33.
60. Litton JK, Rugo HS, Ettl J, Hurvitz SA, Gonçalves A, Lee KH, et al. Talazoparib in Patients with Advanced Breast Cancer and a Germline BRCA Mutation. N Engl J Med. 2018;379(8):753-63.

61. Marabelle A, Le DT, Ascierto PA, Di Giacomo AM, De Jesus-Acosta A, Delord JP, et al. Efficacy of Pembrolizumab in Patients With Noncolorectal High Microsatellite Instability/Mismatch Repair-Deficient Cancer: Results From the Phase II KEYNOTE-158 Study. J Clin Oncol. 2020;38(1):1-10.
62. Carausu M, Bidard FC, Callens C, Melaabi S, Jeannot E, Pierga JY, et al. ESR1 mutations: a new biomarker in breast cancer. Expert Rev Mol Diagn. 2019;19(7):599-611.
63. Hyman DM, Piha-Paul SA, Won H, Rodon J, Saura C, Shapiro GI, et al. HER kinase inhibition in patients with HER2- and HER3-mutant cancers. Nature. 2018;554(7691):189-94.
64. Heitzer E, Ulz P, Geigl JB. Circulating tumor DNA as a liquid biopsy for cancer. Clin Chem. 2015;61(1):112-23.
65. Buono G, Gerratana L, Bulfoni M, Provinciali N, Basile D, Giuliano M, et al. Circulating tumor DNA analysis in breast cancer: Is it ready for prime-time? Cancer Treat Rev. 2019;73:73-83.
66. Heitzer E, Haque IS, Roberts CES, Speicher MR. Current and future perspectives of liquid biopsies in genomics-driven oncology. Nat Rev Genet. 2019;20(2):71-88.
67. Teutsch SM, Bradley LA, Palomaki GE, Haddow JE, Piper M, Calonge N, et al. The Evaluation of Genomic Applications in Practice and Prevention (EGAPP) Initiative: methods of the EGAPP Working Group. Genet Med. 2009;11(1):3-14.
68. Rossi G, Mu Z, Rademaker AW, Austin LK, Strickland KS, Costa RLB, et al. Cell-Free DNA and Circulating Tumor Cells: Comprehensive Liquid Biopsy Analysis in Advanced Breast Cancer. Clin Cancer Res. 2018;24(3):560-8.
69. Haber DA, Velculescu VE. Blood-based analyses of cancer: circulating tumor cells and circulating tumor DNA. Cancer Discov. 2014;4(6):650-61.
70. Cristofanilli M, Budd GT, Ellis MJ, Stopeck A, Matera J, Miller MC, et al. Circulating tumor cells, disease progression, and survival in metastatic breast cancer. N Engl J Med. 2004;351(8):781-91.
71. Lin HK, Zheng S, Williams AJ, Balic M, Groshen S, Scher HI, et al. Portable filter-based microdevice for detection and characterization of circulating tumor cells. Clin Cancer Res. 2010;16(20):5011-8.
72. Gertler R, Rosenberg R, Fuehrer K, Dahm M, Nekarda H, Siewert JR. Detection of circulating tumor cells in blood using an optimized density gradient centrifugation. Recent Results Cancer Res. 2003;162:149-55.
73. Gascoyne PR, Noshari J, Anderson TJ, Becker FF. Isolation of rare cells from cell mixtures by dielectrophoresis. Electrophoresis. 2009;30(8):1388-98.
74. Alix-Panabières C, Vendrell JP, Pellé O, Rebillard X, Riethdorf S, Müller V, et al. Detection and characterization of putative metastatic precursor cells in cancer patients. Clin Chem. 2007;53(3):537-9.

75. Riethdorf S, Fritsche H, Müller V, Rau T, Schindlbeck C, Rack B, et al. Detection of circulating tumor cells in peripheral blood of patients with metastatic breast cancer: a validation study of the CellSearch system. Clin Cancer Res. 2007;13(3):920-8.
76. Attard G, Swennenhuis JF, Olmos D, Reid AH, Vickers E, A'Hern R, et al. Characterization of ERG, AR and PTEN gene status in circulating tumor cells from patients with castration-resistant prostate cancer. Cancer Res. 2009;69(7):2912-8.
77. Allard WJ, Matera J, Miller MC, Repollet M, Connelly MC, Rao C, et al. Tumor cells circulate in the peripheral blood of all major carcinomas but not in healthy subjects or patients with nonmalignant diseases. Clin Cancer Res. 2004;10(20):6897-904.
78. Ignatiadis M, Dawson SJ. Circulating tumor cells and circulating tumor DNA for precision medicine: dream or reality? Ann Oncol. 2014;25(12):2304-13.
79. Thiery JP, Acloque H, Huang RY, Nieto MA. Epithelial-mesenchymal transitions in development and disease. Cell. 2009;139(5):871-90.
80. Sieuwerts AM, Kraan J, Bolt J, van der Spoel P, Elstrodt F, Schutte M, et al. Anti-epithelial cell adhesion molecule antibodies and the detection of circulating normal-like breast tumor cells. J Natl Cancer Inst. 2009;101(1):61-6.
81. Ozkumur E, Shah AM, Ciciliano JC, Emmink BL, Miyamoto DT, Brachtel E, et al. Inertial focusing for tumor antigen-dependent and -independent sorting of rare circulating tumor cells. Sci Transl Med. 2013;5(179):179ra47.
82. Di Carlo D, Irimia D, Tompkins RG, Toner M. Continuous inertial focusing, ordering, and separation of particles in microchannels. Proc Natl Acad Sci U S A. 2007;104(48):18892-7.
83. Danila DC, Heller G, Gignac GA, Gonzalez-Espinoza R, Anand A, Tanaka E, et al. Circulating tumor cell number and prognosis in progressive castration-resistant prostate cancer. Clin Cancer Res. 2007;13(23):7053-8.
84. Stott SL, Lee RJ, Nagrath S, Yu M, Miyamoto DT, Ulkus L, et al. Isolation and characterization of circulating tumor cells from patients with localized and metastatic prostate cancer. Sci Transl Med. 2010;2(25):25ra3.
85. Maheswaran S, Sequist LV, Nagrath S, Ulkus L, Brannigan B, Collura CV, et al. Detection of mutations in EGFR in circulating lung-cancer cells. N Engl J Med. 2008;359(4):366-77.
86. Trapp E, Janni W, Schindlbeck C, Jückstock J, Andergassen U, de Gregorio A, et al. Presence of Circulating Tumor Cells in High-Risk Early Breast Cancer During Follow-Up and Prognosis. J Natl Cancer Inst. 2019;111(4):380-7.
87. Smerage JB, Barlow WE, Hortobagyi GN, Winer EP, Leyland-Jones B, Srkalovic G, et al. Circulating tumor cells and response to chemotherapy in metastatic breast cancer: SWOG S0500. J Clin Oncol. 2014;32(31):3483-9.

88. Scher HI, Heller G, Molina A, Attard G, Danila DC, Jia X, et al. Circulating tumor cell biomarker panel as an individual-level surrogate for survival in metastatic castration-resistant prostate cancer. J Clin Oncol. 2015;33(12):1348-55.
89. Ignatiadis M, Litière S, Rothe F, Riethdorf S, Proudhon C, Fehm T, et al. Trastuzumab versus observation for HER2 nonamplified early breast cancer with circulating tumor cells (EORTC 90091-10093, BIG 1-12, Treat CTC): a randomized phase II trial. Ann Oncol. 2018;29(8):1777-83.
90. Janni W. Clinical utility of repeated circulating tumor cell (CTC) enumeration as early treatment monitoring tool in metastatic breast cancer (MBC) – a global pooled analysis with individual patient data. San Antonio Breast Cancer Symposium, Virtual Meeting Dec 11, 2020; Texas, USA.2020.
91. Schwarzenbach H, Pantel K. Circulating DNA as biomarker in breast cancer. Breast Cancer Res. 2015;17(1):136.
92. Swarup V, Rajeswari MR. Circulating (cell-free) nucleic acids--a promising, non-invasive tool for early detection of several human diseases. FEBS Lett. 2007;581(5):795-9.
93. Kohler C, Barekati Z, Radpour R, Zhong XY. Cell-free DNA in the circulation as a potential cancer biomarker. Anticancer Res. 2011;31(8):2623-8.
94. Jahr S, Hentze H, Englisch S, Hardt D, Fackelmayer FO, Hesch RD, et al. DNA fragments in the blood plasma of cancer patients: quantitations and evidence for their origin from apoptotic and necrotic cells. Cancer Res. 2001;61(4):1659-65.
95. Beaver JA, Jelovac D, Balukrishna S, Cochran R, Croessmann S, Zabransky DJ, et al. Detection of cancer DNA in plasma of patients with early-stage breast cancer. Clin Cancer Res. 2014;20(10):2643-50.
96. Diehl F, Schmidt K, Choti MA, Romans K, Goodman S, Li M, et al. Circulating mutant DNA to assess tumor dynamics. Nat Med. 2008;14(9):985-90.
97. Anker P, Lyautey J, Lederrey C, Stroun M. Circulating nucleic acids in plasma or serum. Clin Chim Acta. 2001;313(1-2):143-6.
98. Vasioukhin V, Anker P, Maurice P, Lyautey J, Lederrey C, Stroun M. Point mutations of the N-ras gene in the blood plasma DNA of patients with myelodysplastic syndrome or acute myelogenous leukaemia. Br J Haematol. 1994;86(4):774-9.
99. Milbury CA, Zhong Q, Lin J, Williams M, Olson J, Link DR, et al. Determining lower limits of detection of digital PCR assays for cancer-related gene mutations. Biomol Detect Quantif. 2014;1(1):8-22.
100. Hindson BJ, Ness KD, Masquelier DA, Belgrader P, Heredia NJ, Makarewicz AJ, et al. High-throughput droplet digital PCR system for absolute quantitation of DNA copy number. Anal Chem. 2011;83(22):8604-10.

101. Diehl F, Li M, He Y, Kinzler KW, Vogelstein B, Dressman D. BEAMing: single-molecule PCR on microparticles in water-in-oil emulsions. Nat Methods. 2006;3(7):551-9.
102. Herman JG, Graff JR, Myöhänen S, Nelkin BD, Baylin SB. Methylation-specific PCR: a novel PCR assay for methylation status of CpG islands. Proc Natl Acad Sci U S A. 1996;93(18):9821-6.
103. Thompson JC, Yee SS, Troxel AB, Savitch SL, Fan R, Balli D, et al. Detection of Therapeutically Targetable Driver and Resistance Mutations in Lung Cancer Patients by Next-Generation Sequencing of Cell-Free Circulating Tumor DNA. Clin Cancer Res. 2016;22(23):5772-82.
104. Forshew T, Murtaza M, Parkinson C, Gale D, Tsui DW, Kaper F, et al. Noninvasive identification and monitoring of cancer mutations by targeted deep sequencing of plasma DNA. Sci Transl Med. 2012;4(136):136ra68.
105. Kinde I, Wu J, Papadopoulos N, Kinzler KW, Vogelstein B. Detection and quantification of rare mutations with massively parallel sequencing. Proc Natl Acad Sci U S A. 2011;108(23):9530-5.
106. Leary RJ, Kinde I, Diehl F, Schmidt K, Clouser C, Duncan C, et al. Development of personalized tumor biomarkers using massively parallel sequencing. Sci Transl Med. 2010;2(20):20ra14.
107. Wang TL, Rago C, Silliman N, Ptak J, Markowitz S, Willson JK, et al. Prevalence of somatic alterations in the colorectal cancer cell genome. Proc Natl Acad Sci U S A. 2002;99(5):3076-80.
108. Jeselsohn R, Buchwalter G, De Angelis C, Brown M, Schiff R. ESR1 mutations—a mechanism for acquired endocrine resistance in breast cancer. Nat Rev Clin Oncol. 2015;12(10):573-83.
109. Chu D, Paoletti C, Gersch C, VanDenBerg DA, Zabransky DJ, Cochran RL, et al. ESR1 Mutations in Circulating Plasma Tumor DNA from Metastatic Breast Cancer Patients. Clin Cancer Res. 2016;22(4):993-9.
110. Robinson DR, Wu YM, Vats P, Su F, Lonigro RJ, Cao X, et al. Activating ESR1 mutations in hormone-resistant metastatic breast cancer. Nat Genet. 2013;45(12):1446-51.
111. Schiavon G, Hrebien S, Garcia-Murillas I, Cutts RJ, Pearson A, Tarazona N, et al. Analysis of ESR1 mutation in circulating tumor DNA demonstrates evolution during therapy for metastatic breast cancer. Sci Transl Med. 2015;7(313):313ra182.
112. Johnston SR, Kilburn LS, Ellis P, Dodwell D, Cameron D, Hayward L, et al. Fulvestrant plus anastrozole or placebo versus exemestane alone after progression on non-steroidal aromatase inhibitors in postmenopausal patients with hormone-receptor-positive locally advanced or metastatic breast cancer (SoFEA): a composite, multicentre, phase 3 randomised trial. Lancet Oncol. 2013;14(10):989-98.

113. Fribbens C, O'Leary B, Kilburn L, Hrebien S, Garcia-Murillas I, Beaney M, et al. Plasma ESR1 Mutations and the Treatment of Estrogen Receptor-Positive Advanced Breast Cancer. J Clin Oncol. 2016;34(25):2961-8.
114. Chandarlapaty S, Chen D, He W, Sung P, Samoila A, You D, et al. Prevalence of ESR1 Mutations in Cell-Free DNA and Outcomes in Metastatic Breast Cancer: A Secondary Analysis of the BOLERO-2 Clinical Trial. JAMA Oncol. 2016;2(10):1310-5.
115. O'Leary B, Hrebien S, Morden JP, Beaney M, Fribbens C, Huang X, et al. Early circulating tumor DNA dynamics and clonal selection with palbociclib and fulvestrant for breast cancer. Nat Commun. 2018;9(1):896.
116. Turner NC, Kingston B, Kilburn LS, Kernaghan S, Wardley AM, Macpherson IR, et al. Circulating tumour DNA analysis to direct therapy in advanced breast cancer (plasmaMATCH): a multicentre, multicohort, phase 2a, platform trial. Lancet Oncol. 2020;21(10):1296-308.
117. Garcia-Murillas I, Schiavon G, Weigelt B, Ng C, Hrebien S, Cutts RJ, et al. Mutation tracking in circulating tumor DNA predicts relapse in early breast cancer. Sci Transl Med. 2015;7(302):302ra133.
118. Cohen JD, Li L, Wang Y, Thoburn C, Afsari B, Danilova L, et al. Detection and localization of surgically resectable cancers with a multi-analyte blood test. Science. 2018;359(6378):926-30.
119. Kalinich M, Haber DA. Cancer detection: Seeking signals in blood. Science. 2018;359(6378):866-7.
120. Dawson SJ, Tsui DW, Murtaza M, Biggs H, Rueda OM, Chin SF, et al. Analysis of circulating tumor DNA to monitor metastatic breast cancer. N Engl J Med. 2013;368(13):1199-209.
121. Shiomi-Mouri Y, Kousaka J, Ando T, Tetsuka R, Nakano S, Yoshida M, et al. Clinical significance of circulating tumor cells (CTCs) with respect to optimal cut-off value and tumor markers in advanced/metastatic breast cancer. Breast Cancer. 2016;23(1):120-7.
122. Bidard FC, Mathiot C, Delaloge S, Brain E, Giachetti S, de Cremoux P, et al. Single circulating tumor cell detection and overall survival in nonmetastatic breast cancer. Ann Oncol. 2010;21(4):729-33.
123. Fehm T, Sauerbrei W. Information from CTC measurements for metastatic breast cancer prognosis-we should do more than selecting an "optimal cut point". Breast Cancer Res Treat. 2010;122(1):219-20.
124. Hayes DF, Cristofanilli M, Budd GT, Ellis MJ, Stopeck A, Miller MC, et al. Circulating tumor cells at each follow-up time point during therapy of metastatic breast cancer patients predict progression-free and overall survival. Clin Cancer Res. 2006;12(14 Pt 1):4218-24.

125. Olsson E, Winter C, George A, Chen Y, Howlin J, Tang MH, et al. Serial monitoring of circulating tumor DNA in patients with primary breast cancer for detection of occult metastatic disease. EMBO Mol Med. 2015;7(8):1034-47.
126. Shaw JA, Guttery DS, Hills A, Fernandez-Garcia D, Page K, Rosales BM, et al. Mutation Analysis of Cell-Free DNA and Single Circulating Tumor Cells in Metastatic Breast Cancer Patients with High Circulating Tumor Cell Counts. Clin Cancer Res. 2017;23(1):88-96.
127. Bettegowda C, Sausen M, Leary RJ, Kinde I, Wang Y, Agrawal N, et al. Detection of circulating tumor DNA in early- and late-stage human malignancies. Sci Transl Med. 2014;6(224):224ra24.
128. de Bono JS, Scher HI, Montgomery RB, Parker C, Miller MC, Tissing H, et al. Circulating tumor cells predict survival benefit from treatment in metastatic castration-resistant prostate cancer. Clin Cancer Res. 2008;14(19):6302-9.
129. Siravegna G, Marsoni S, Siena S, Bardelli A. Integrating liquid biopsies into the management of cancer. Nat Rev Clin Oncol. 2017;14(9):531-48.
130. Suppan C, Brcic I, Tiran V, Mueller HD, Posch F, Auer M, et al. Untargeted Assessment of Tumor Fractions in Plasma for Monitoring and Prognostication from Metastatic Breast Cancer Patients Undergoing Systemic Treatment. Cancers (Basel). 2019;11(8).
131. Belic J, Koch M, Ulz P, Auer M, Gerhalter T, Mohan S, et al. Rapid Identification of Plasma DNA Samples with Increased ctDNA Levels by a Modified FAST-SeqS Approach. Clin Chem. 2015;61(6):838-49.
132. Heitzer E, Ulz P, Belic J, Gutschi S, Quehenberger F, Fischereder K, et al. Tumor-associated copy number changes in the circulation of patients with prostate cancer identified through whole-genome sequencing. Genome Med. 2013;5(4):30.
133. Ulz P, Belic J, Graf R, Auer M, Lafer I, Fischereder K, et al. Whole-genome plasma sequencing reveals focal amplifications as a driving force in metastatic prostate cancer. Nat Commun. 2016;7:12008.
134. Adalsteinsson VA, Ha G, Freeman SS, Choudhury AD, Stover DG, Parsons HA, et al. Scalable whole-exome sequencing of cell-free DNA reveals high concordance with metastatic tumors. Nat Commun. 2017;8(1):1324.
135. Zheng S, Lin H, Liu JQ, Balic M, Datar R, Cote RJ, et al. Membrane microfilter device for selective capture, electrolysis and genomic analysis of human circulating tumor cells. J Chromatogr A. 2007;1162(2):154-61.
136. Schemper M, Smith TL. A note on quantifying follow-up in studies of failure time. Control Clin Trials. 1996;17(4):343-6.
137. Stahlberg A, Krzyzanowski PM, Egyud M, Filges S, Stein L, Godfrey TE. Simple multiplexed PCR-based barcoding of DNA for ultrasensitive mutation detection by next-generation sequencing. Nat Protoc. 2017;12(4):664-82.

138. Wang K, Li M, Hakonarson H. ANNOVAR: functional annotation of genetic variants from high-throughput sequencing data. Nucleic Acids Res. 2010;38(16):e164.
139. Cingolani P, Platts A, Wang le L, Coon M, Nguyen T, Wang L, et al. A program for annotating and predicting the effects of single nucleotide polymorphisms, SnpEff: SNPs in the genome of Drosophila melanogaster strain w1118; iso-2; iso-3. Fly (Austin). 2012;6(2):80-92.
140. Vasan N, Razavi P, Johnson JL, Shao H, Shah H, Antoine A, et al. Double PIK3CA mutations in cis increase oncogenicity and sensitivity to PI3Kalpha inhibitors. Science. 2019;366(6466):714-23.
141. Belic J, Graf R, Bauernhofer T, Cherkas Y, Ulz P, Waldispuehl-Geigl J, et al. Genomic alterations in plasma DNA from patients with metastasized prostate cancer receiving abiraterone or enzalutamide. International journal of cancer Journal international du cancer. 2018.
142. Stover DG, Parsons HA, Ha G, Freeman SS, Barry WT, Guo H, et al. Association of Cell-Free DNA Tumor Fraction and Somatic Copy Number Alterations With Survival in Metastatic Triple-Negative Breast Cancer. J Clin Oncol. 2018;36(6):543-53.
143. Annala M, Vandekerkhove G, Khalaf D, Taavitsainen S, Beja K, Warner EW, et al. Circulating Tumor DNA Genomics Correlate with Resistance to Abiraterone and Enzalutamide in Prostate Cancer. Cancer discovery. 2018;8(4):444-57.
144. Lee RJ, Gremel G, Marshall A, Myers KA, Fisher N, Dunn JA, et al. Circulating tumor DNA predicts survival in patients with resected high-risk stage II/III melanoma. Ann Oncol. 2018;29(2):490-6.
145. Tie J, Kinde I, Wang Y, Wong HL, Roebert J, Christie M, et al. Circulating tumor DNA as an early marker of therapeutic response in patients with metastatic colorectal cancer. Ann Oncol. 2015;26(8):1715-22.
146. Yates LR, Knappskog S, Wedge D, Farmery JHR, Gonzalez S, Martincorena I, et al. Genomic Evolution of Breast Cancer Metastasis and Relapse. Cancer Cell. 2017;32(2):169-84 e7.
147. Douville C, Springer S, Kinde I, Cohen JD, Hruban RH, Lennon AM, et al. Detection of aneuploidy in patients with cancer through amplification of long interspersed nucleotide elements (LINEs). Proc Natl Acad Sci U S A. 2018;115(8):1871-6.
148. Baselga J, Im SA, Iwata H, Cortes J, De Laurentiis M, Jiang Z, et al. Buparlisib plus fulvestrant versus placebo plus fulvestrant in postmenopausal, hormone receptor-positive, HER2-negative, advanced breast cancer (BELLE-2): a randomised, double-blind, placebo-controlled, phase 3 trial. Lancet Oncol. 2017;18(7):904-16.
149. Baselga J, Dent SF, Cortés J, Im Y-H, Diéras V, Harbeck N, et al. Phase III study of taselisib (GDC-0032) + fulvestrant (FULV) v FULV in patients (pts) with estrogen receptor (ER)-positive, PIK3CA-mutant (MUT), locally advanced or metastatic breast cancer (MBC):

Primary analysis from SANDPIPER. Journal of Clinical Oncology. 2018;36(18_suppl):LBA1006-LBA.
150. Baselga J, Sellami D, El-Hashimy M, Dharan B, Wang A, Scheuer N, et al. Abstract A050: PIK3CA mutation status in tumor tissue and ctDNA as a biomarker for PFS in patients with HR+, HER2- ABC treated with buparlisib or placebo plus fulvestrant: results from the BELLE-2 and BELLE-3 randomized studies. Molecular Cancer Therapeutics. 2018;17(1 Supplement):A050-A.
151. Martinez-Saez O, Chic N, Pascual T, Adamo B, Vidal M, Gonzalez-Farre B, et al. Frequency and spectrum of PIK3CA somatic mutations in breast cancer. Breast Cancer Res. 2020;22(1):45.
152. Juric D, Ciruelos E, Rubovszky G, Campone M, Loibl S, Rugo H, et al. Abstract GS3-08: Alpelisib + fulvestrant for advanced breast cancer: Subgroup analyses from the phase III SOLAR-1 trial. Cancer Research. 2019;79(4 Supplement):GS3-08-GS3-.
153. Dandachi N, Posch F, Graf R, Suppan C, Klocker EV, Müller HD, et al. Longitudinal tumor fraction trajectories predict risk of progression in metastatic HR+ breast cancer patients undergoing CDK4/6 treatment. Mol Oncol. 2020.
154. Tzanikou E, Markou A, Politaki E, Koutsopoulos A, Psyrri A, Mavroudis D, et al. PIK3CA hotspot mutations in circulating tumor cells and paired circulating tumor DNA in breast cancer: a direct comparison study. Mol Oncol. 2019;13(12):2515-30.
155. Markou A, Farkona S, Schiza C, Efstathiou T, Kounelis S, Malamos N, et al. PIK3CA mutational status in circulating tumor cells can change during disease recurrence or progression in patients with breast cancer. Clin Cancer Res. 2014;20(22):5823-34.
156. Bi L, Okabe I, Bernard DJ, Wynshaw-Boris A, Nussbaum RL. Proliferative defect and embryonic lethality in mice homozygous for a deletion in the p110alpha subunit of phosphoinositide 3-kinase. J Biol Chem. 1999;274(16):10963-8.
157. O'Leary B, Cutts RJ, Liu Y, Hrebien S, Huang X, Fenwick K, et al. The Genetic Landscape and Clonal Evolution of Breast Cancer Resistance to Palbociclib plus Fulvestrant in the PALOMA-3 Trial. Cancer Discov. 2018;8(11):1390-403.